

Electronic Supplementary Information for:

Linker design for the modular assembly of multifunctional and targeted platinum(II)-containing anticancer agents

Song Ding and Ulrich Bierbach

Department of Chemistry, Wake Forest University, Winston-Salem, North Carolina 27109,
United States

Content	Page
S1. NMR SPECTROSCOPY	
Figs. S1-S8	S3-S10
S2. LC-MS ANALYSIS OF PURIFIED COMPOUNDS	
Figs. S9-S12	S11-S14
S3. LC-MS ANALYSIS OF COUPLING REACTIONS	
Figs. S13-S27	S15-S29
S4. LC-MS STUDY OF ESTER REACTIVITY	
Figs. S28-S39	S30-S41
S5. SUPPLEMENTARY TABLES	
Table S1. Conversion Yields and HR-ESMS Results for Conjugates	S42
Table S2. Summary of Coupling Reagents Used	S43
	S2

S1. NMR SPECTROSCOPY

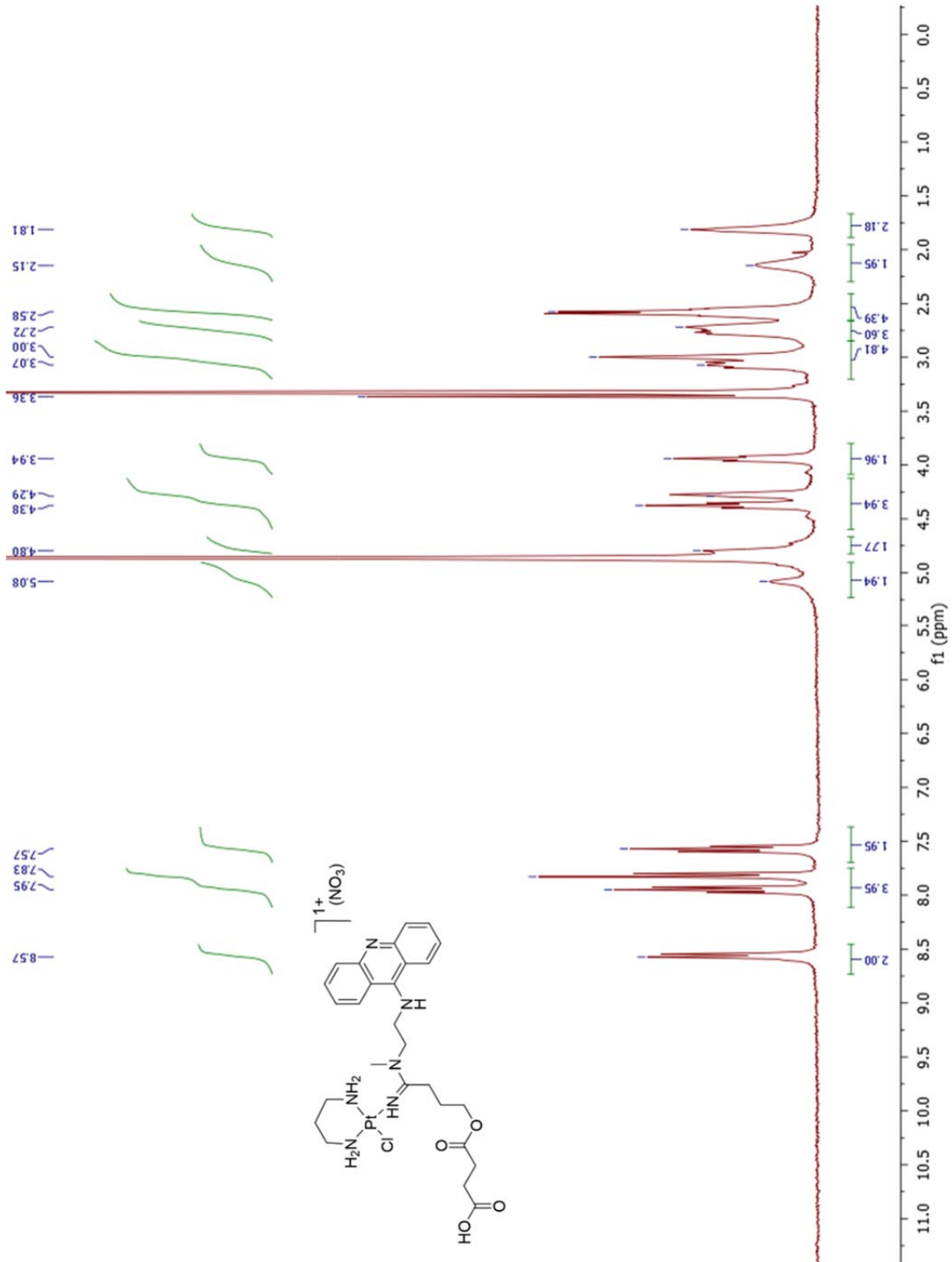


Figure S1. ^1H NMR spectrum of **P1** in $\text{MeOH}-d_4$.

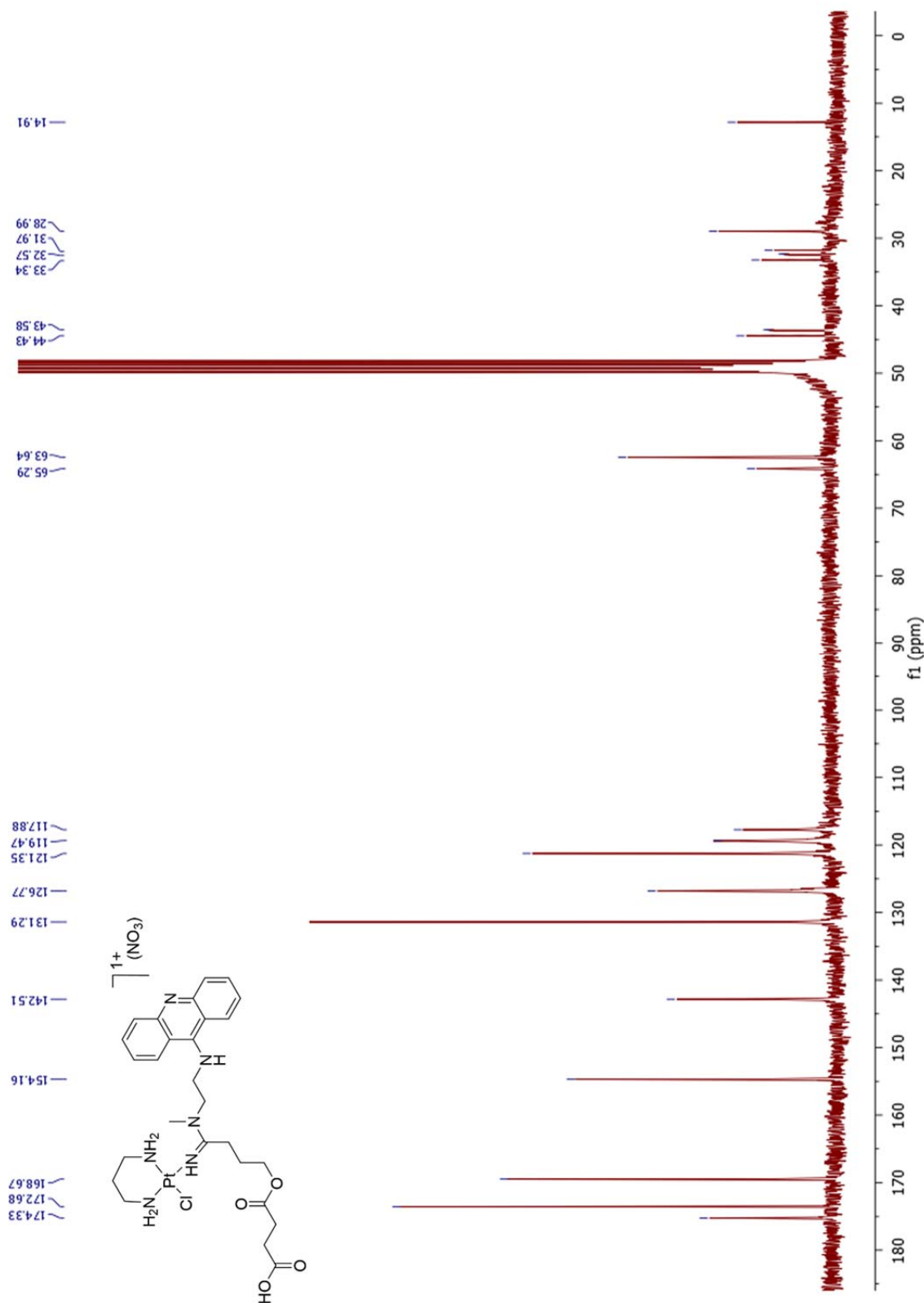


Figure S2. ¹³C NMR spectrum of **P1** in MeOH-*d*₄.

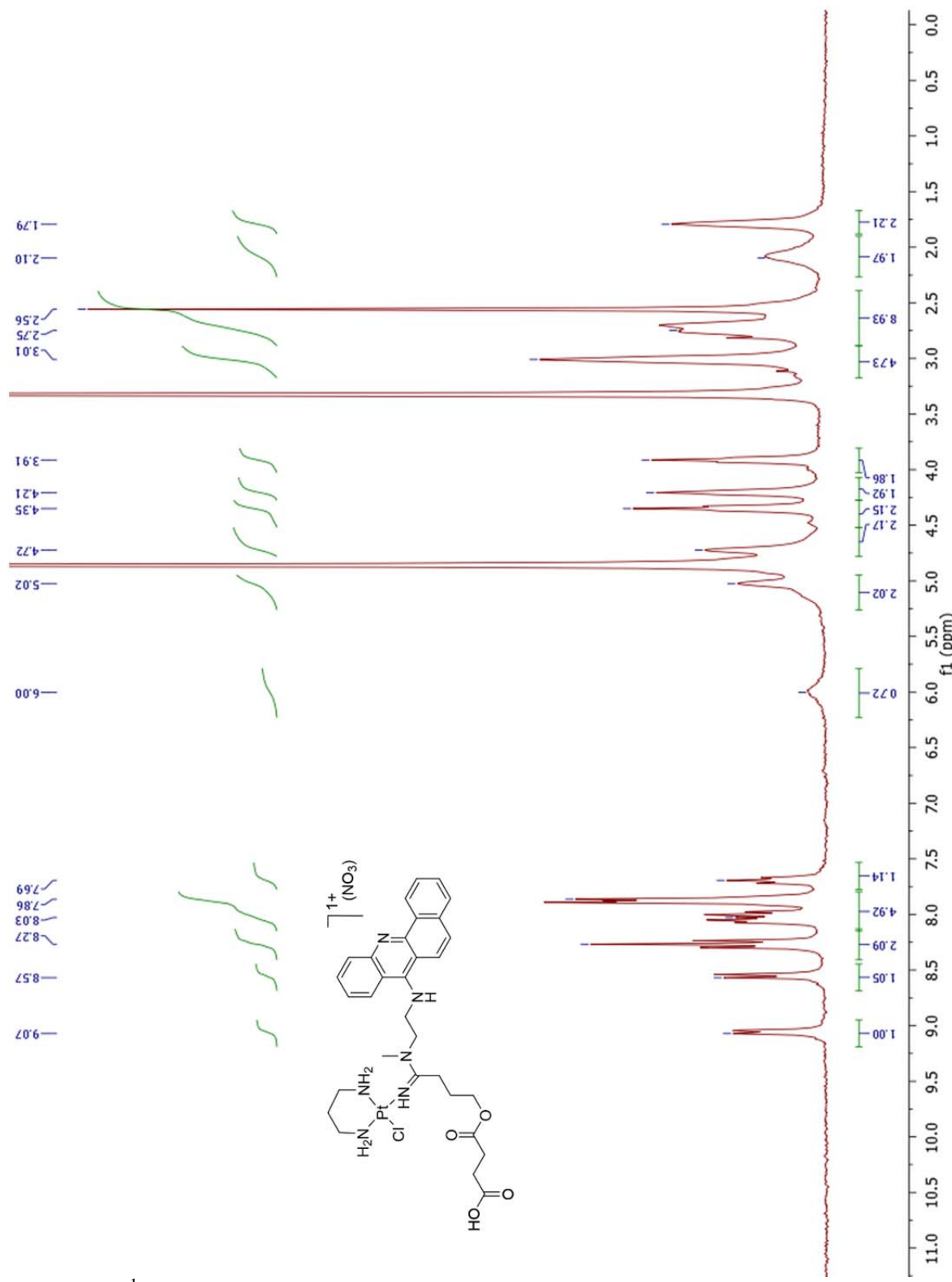


Figure S3. ^1H NMR spectrum of **P2** in $\text{MeOH}-d_4$.

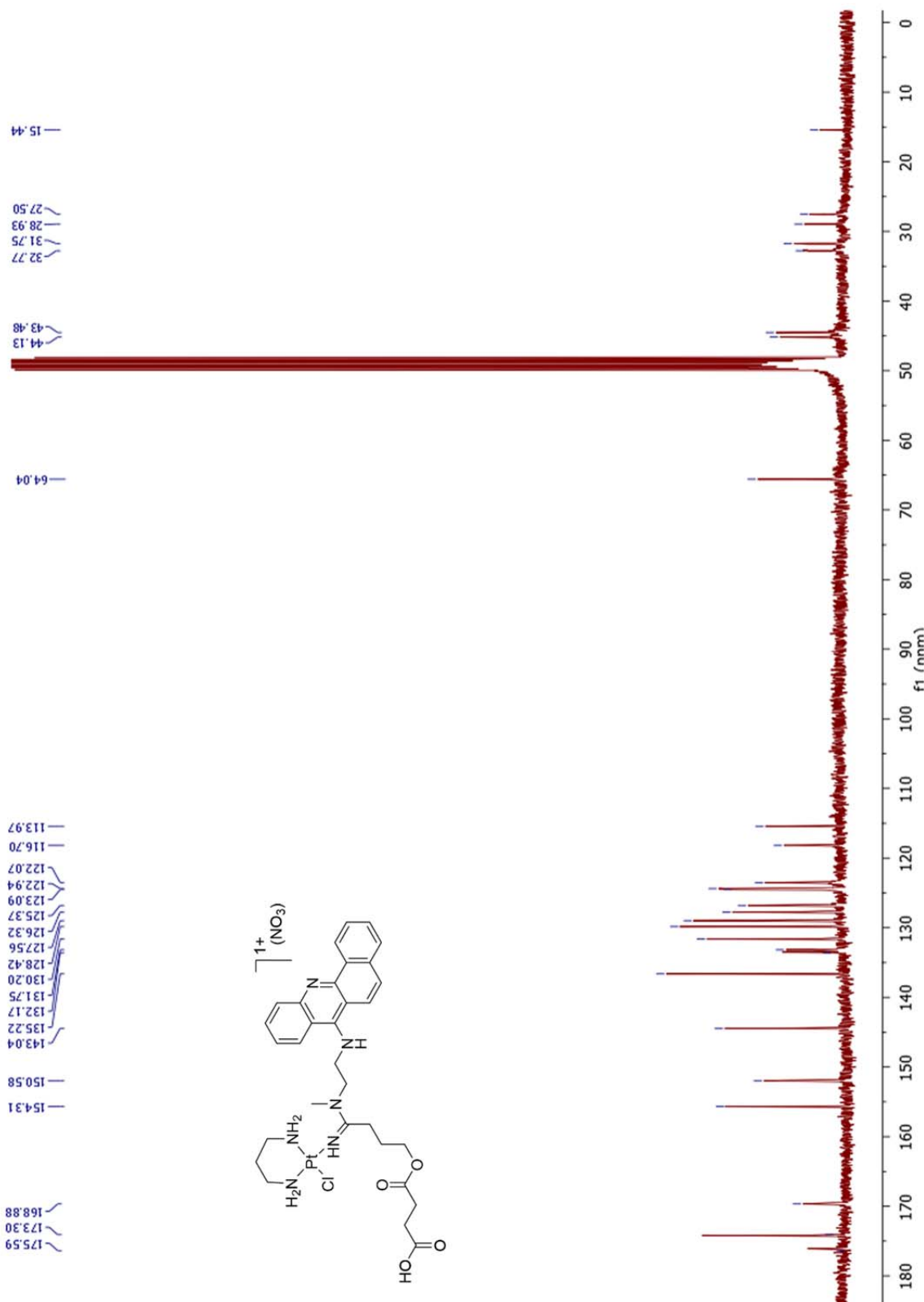
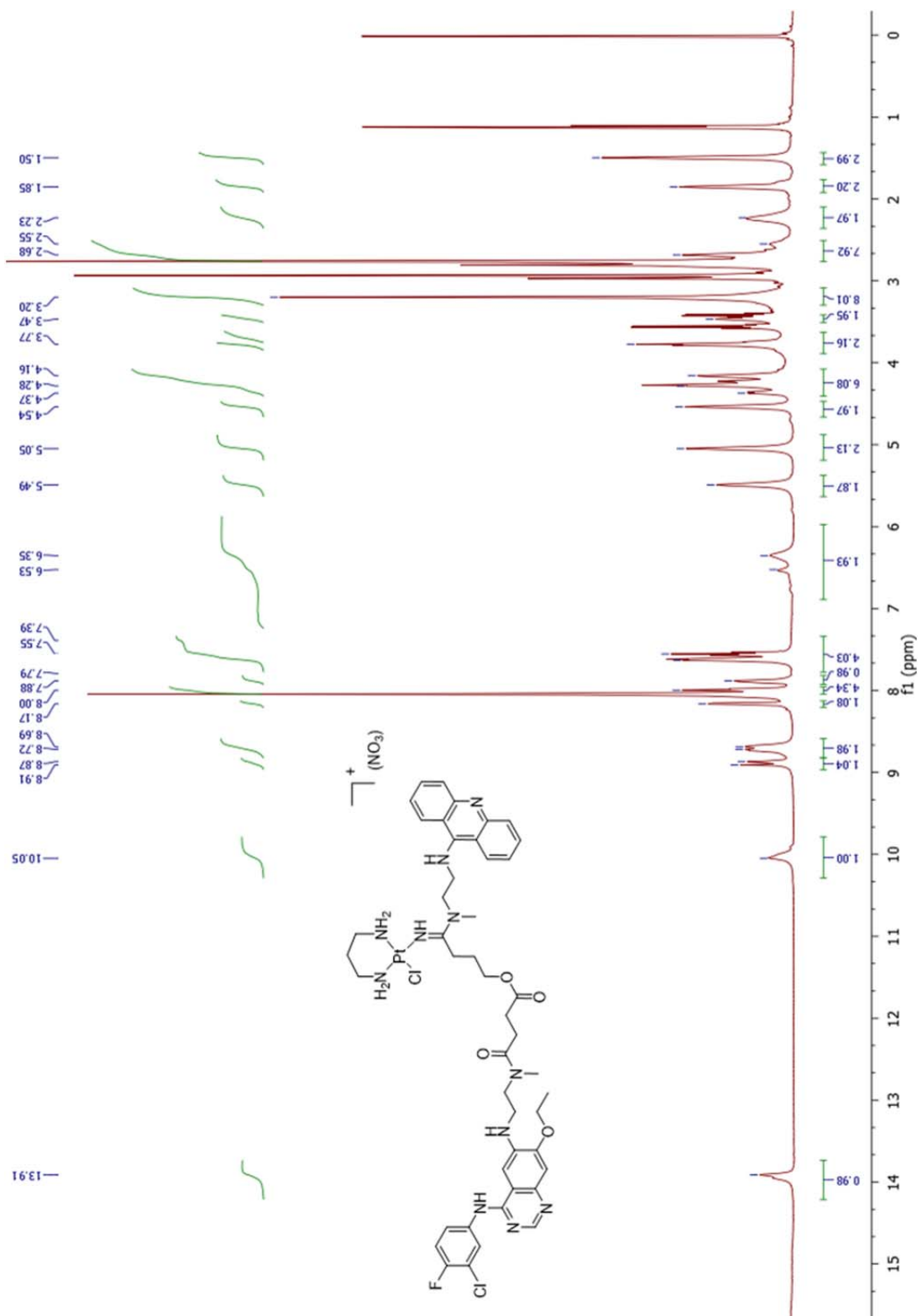


Figure S4. ^{13}C NMR spectrum of **P2** in $\text{MeOH-}d_4$.



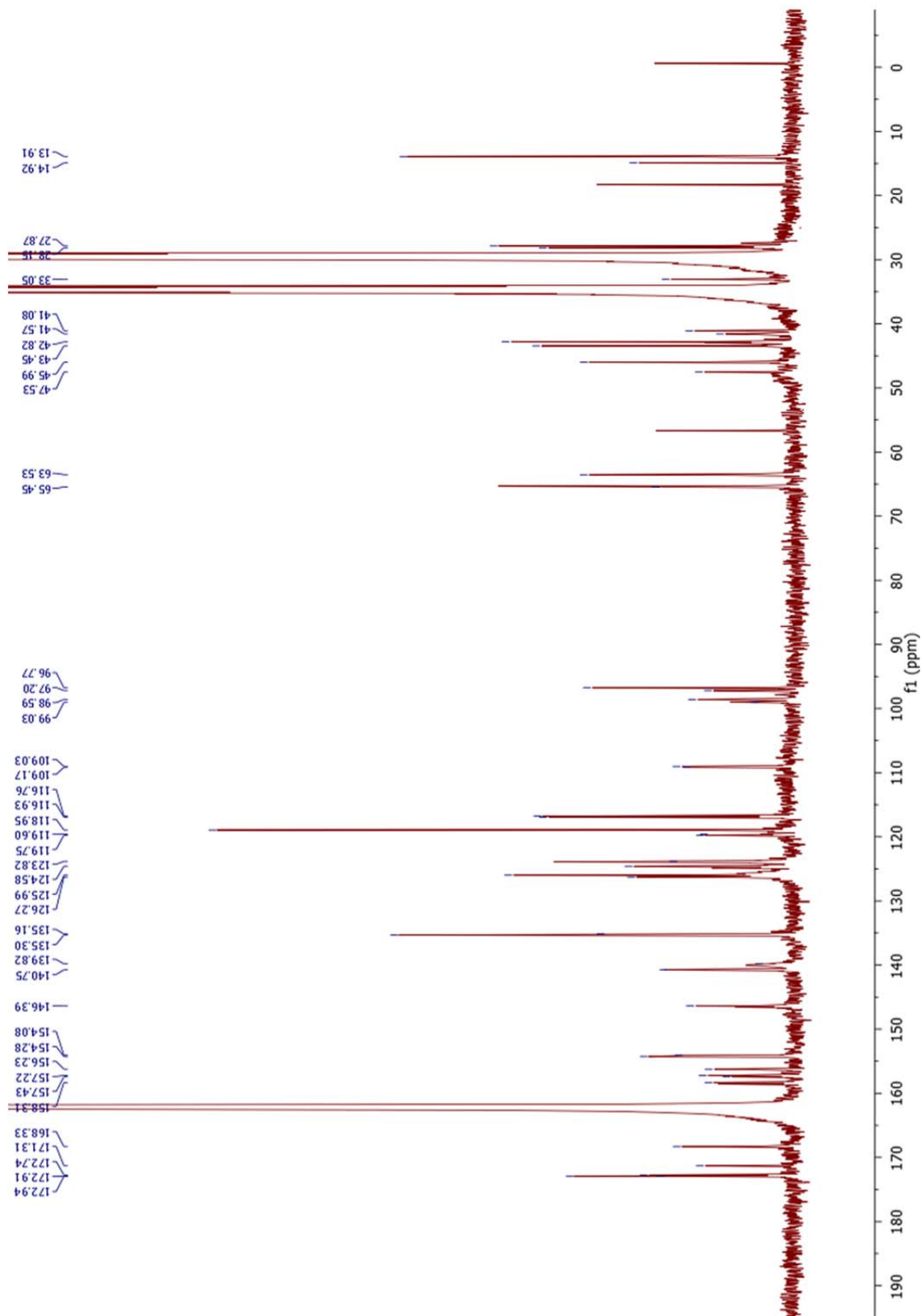


Figure S6. ¹³C NMR spectrum of **P1-N7** in DMF-*d*₇.

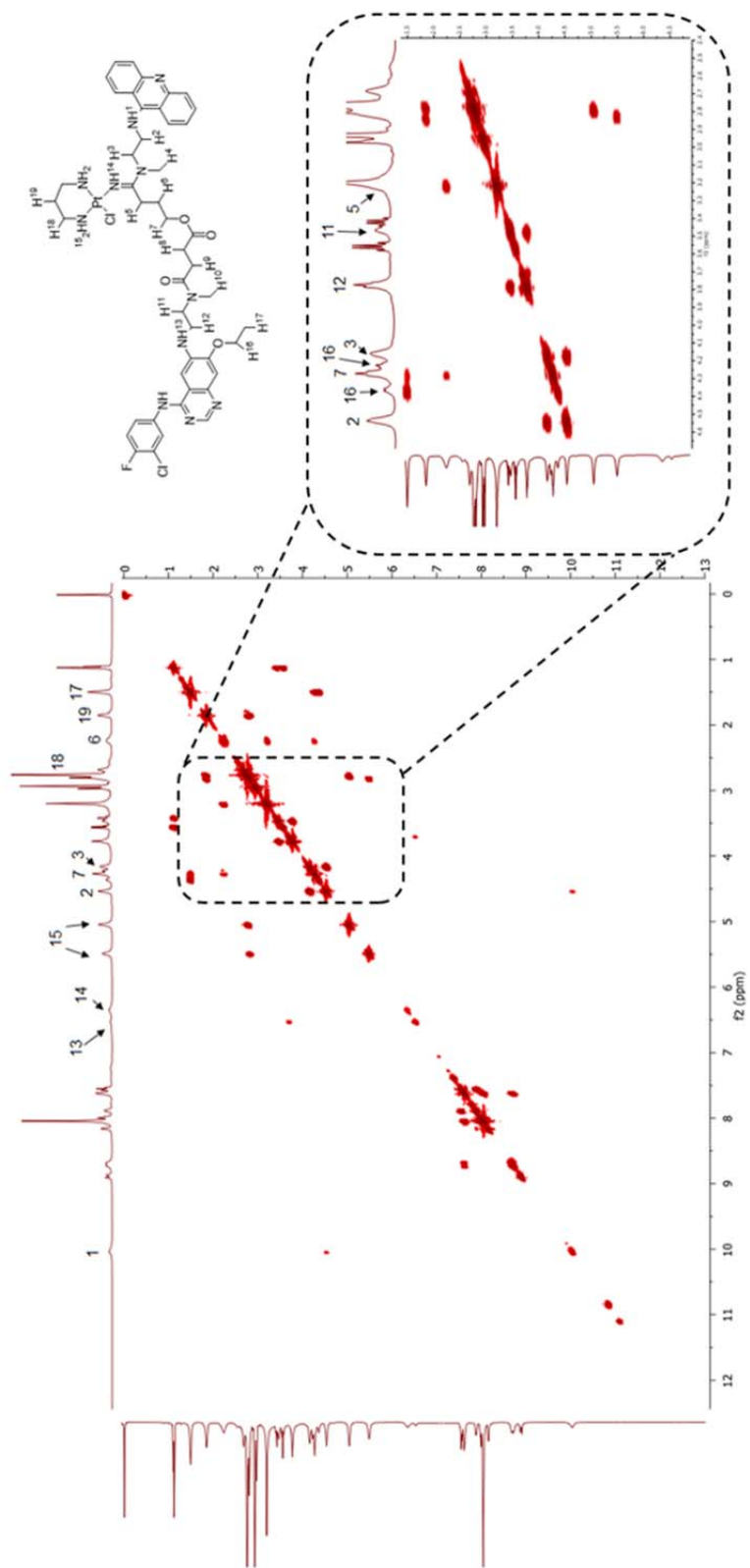


Figure S7. ^1H - ^1H COSY spectrum of compound **P1-N7** in $\text{DMF}-d_7$.

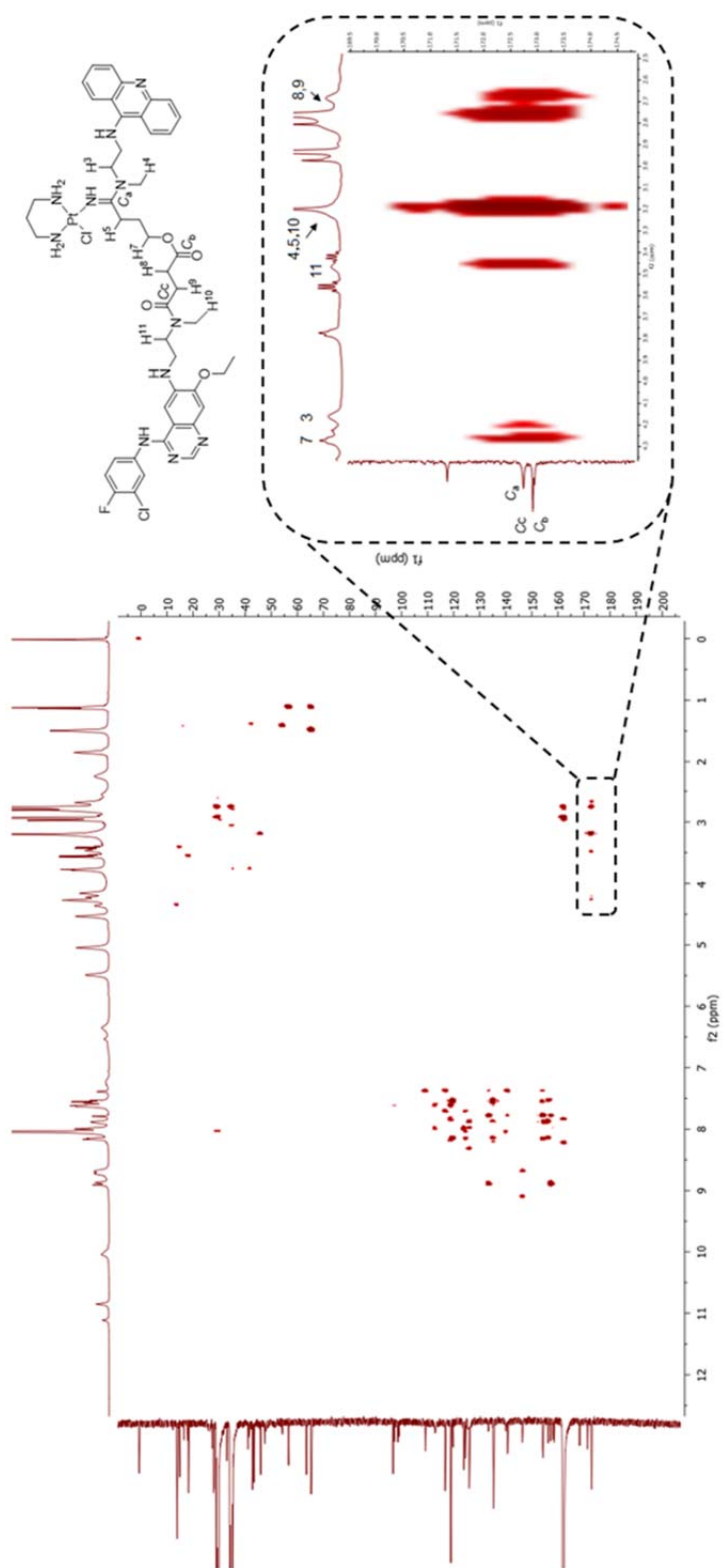


Figure S8. ^1H - ^{13}C HMBC spectrum of compound **P1-N7** in $\text{DMF}-d_7$.

S2. LC-MS ANALYSIS OF PURIFIED COMPOUNDS

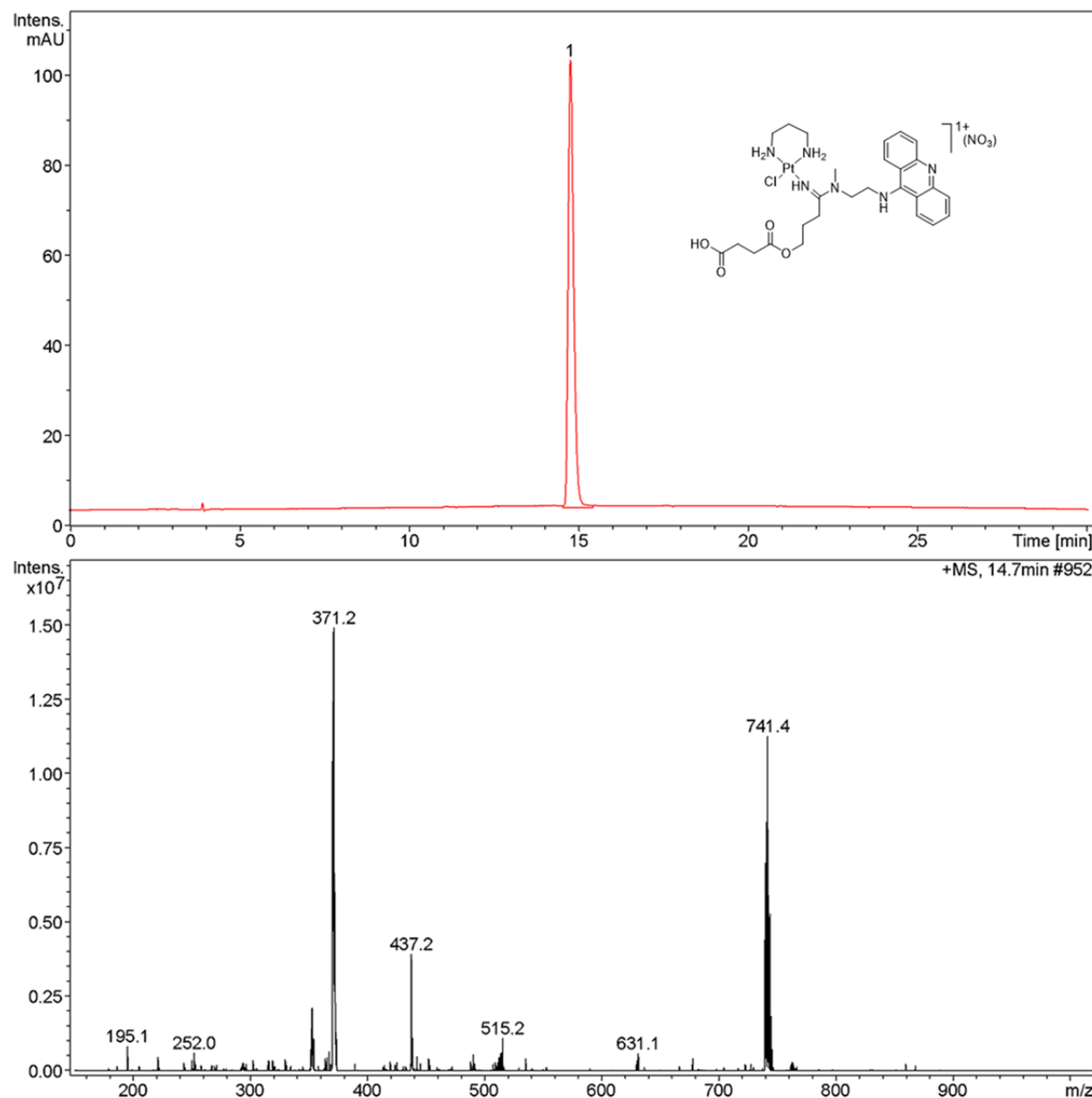


Figure S9. LC-MS analysis of purified **P1**.

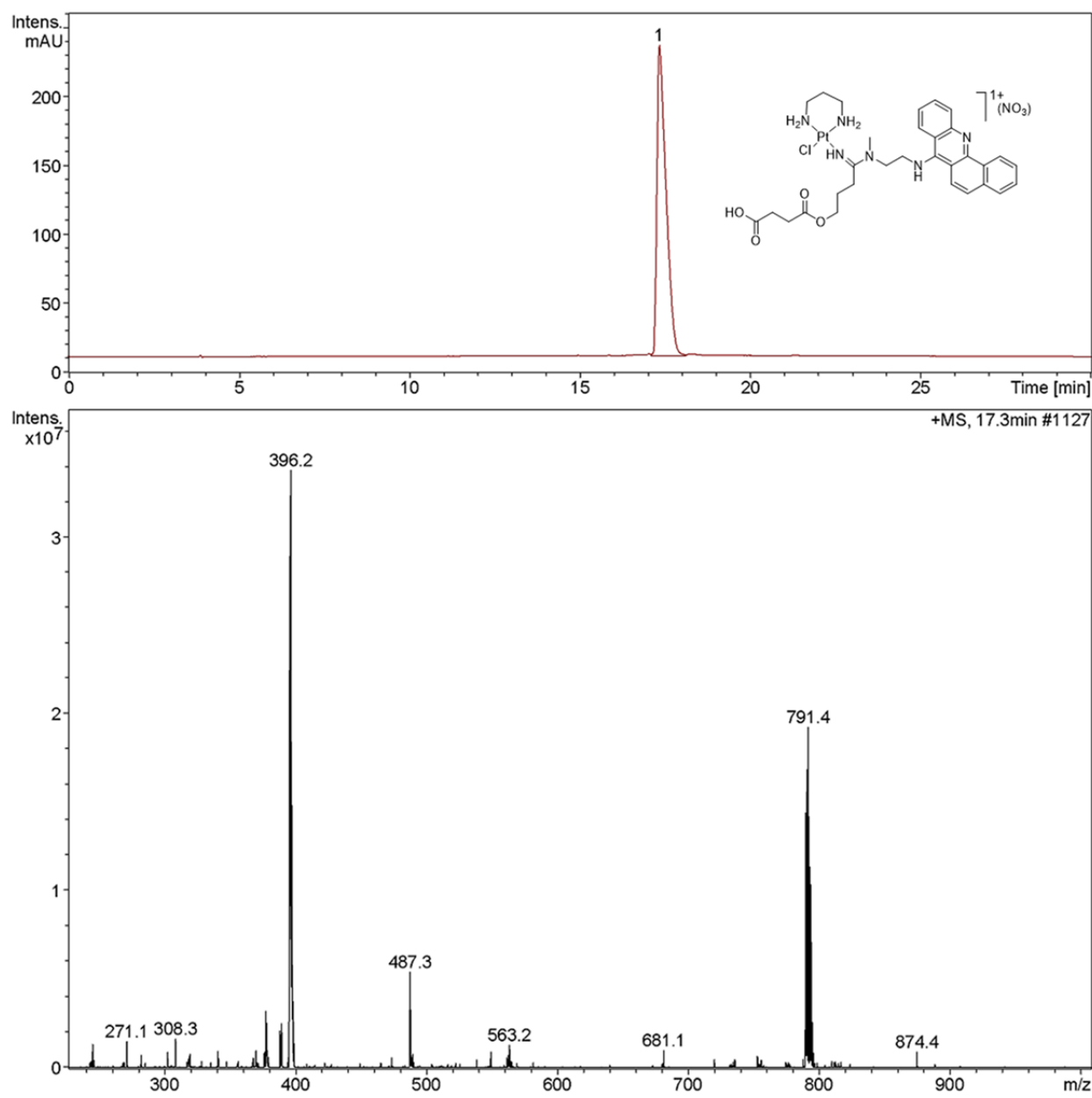


Figure S10. LC-MS analysis of purified **P2**.

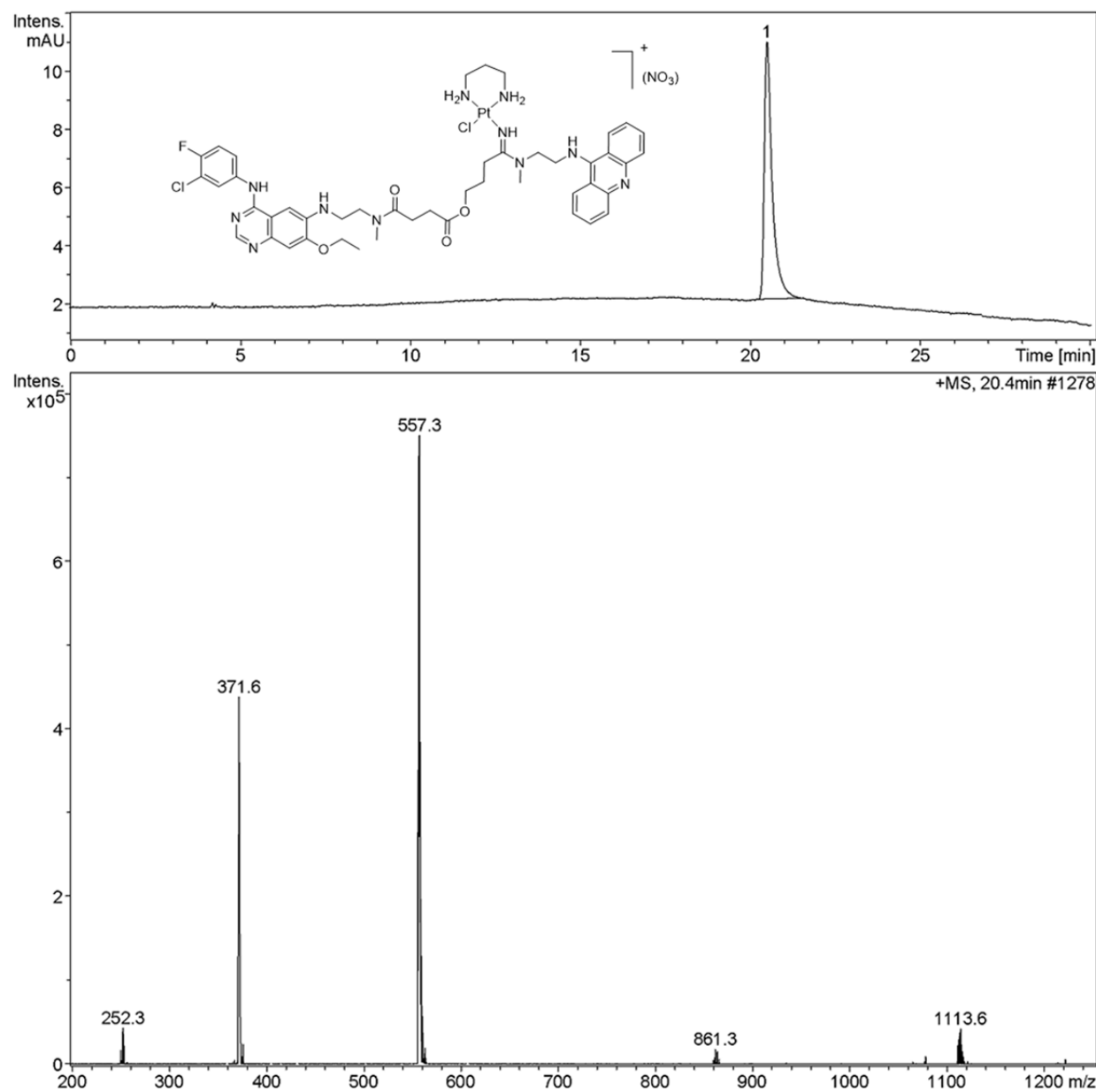


Figure S11. LC-MS analysis of purified **P1-N7**.

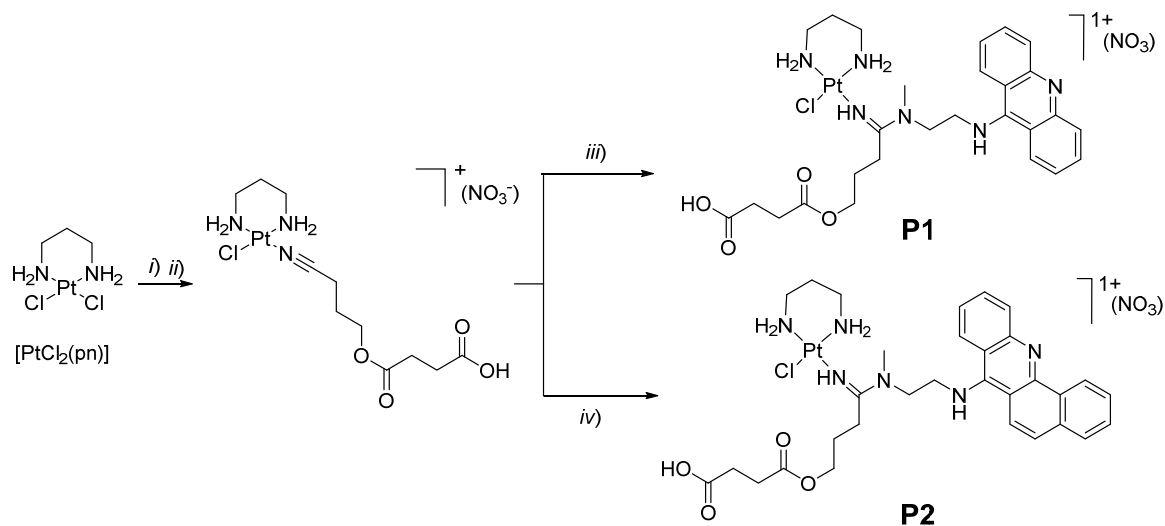


Figure S12. Synthesis of **P1** and **P2**. i) AgNO_3 , DMF, rt, ii) $\text{HOOC}(\text{CH}_2)_2\text{C}(\text{O})\text{O}(\text{CH}_2)_3\text{CN}$ (**3**), DMF, 60°C , 4 h, iii) $\text{N}^1\text{-}(\text{acridin}-9\text{-yl})\text{-N}^2\text{-methylethane-1,2-diamine}$ (**A1**), DMF, 4°C , iv) $\text{N}^1\text{-}(\text{benzo}[c]\text{acridin}-7\text{-yl})\text{-N}^2\text{-methylethane-1,2-diamine}$ (**B1**), DMF, 4°C .

S3. LC-MS ANALYSIS OF COUPLING REACTIONS

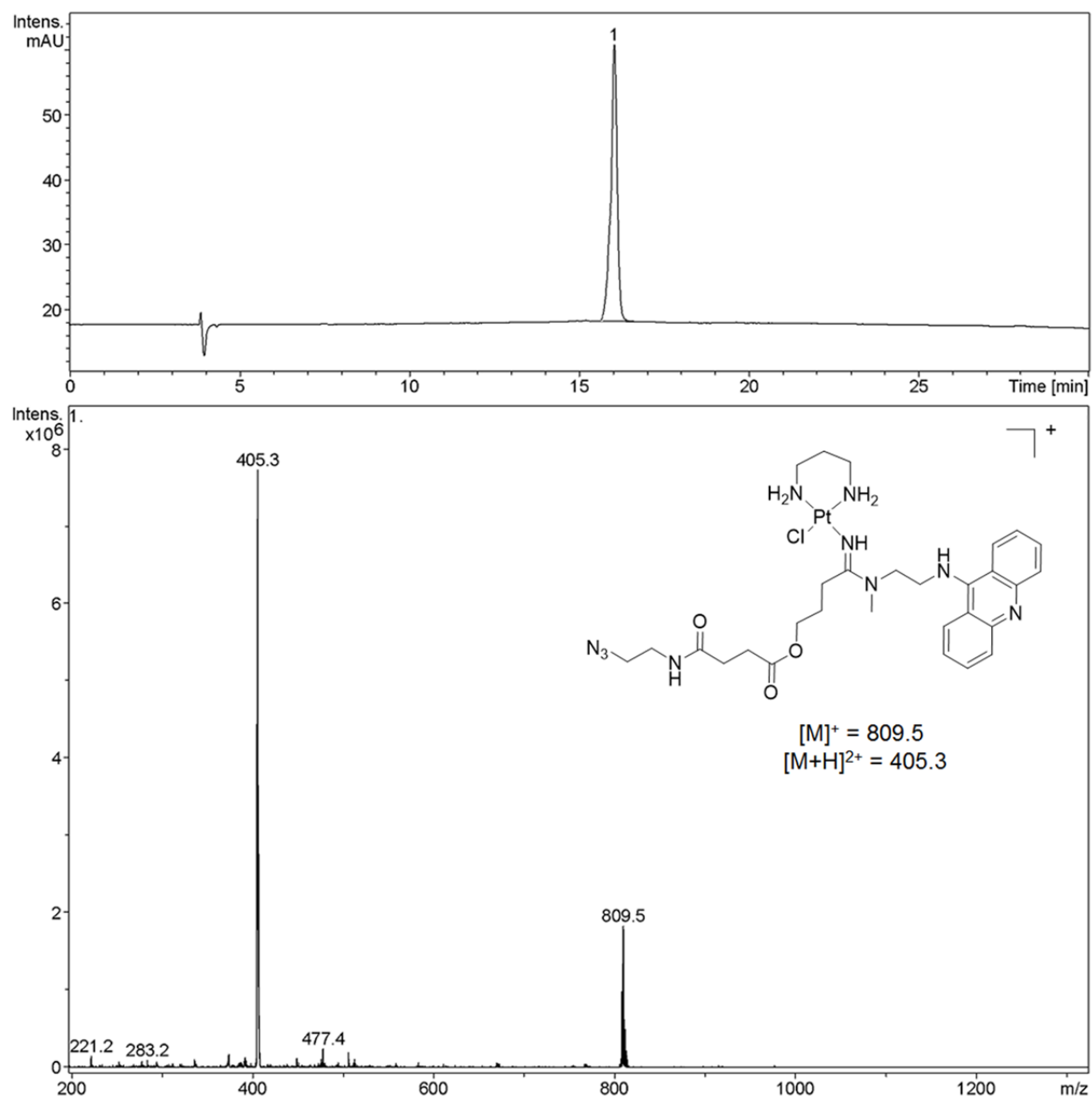


Figure S13. LC-MS analysis of the reaction mixture for the preparation of **P1-N1**.

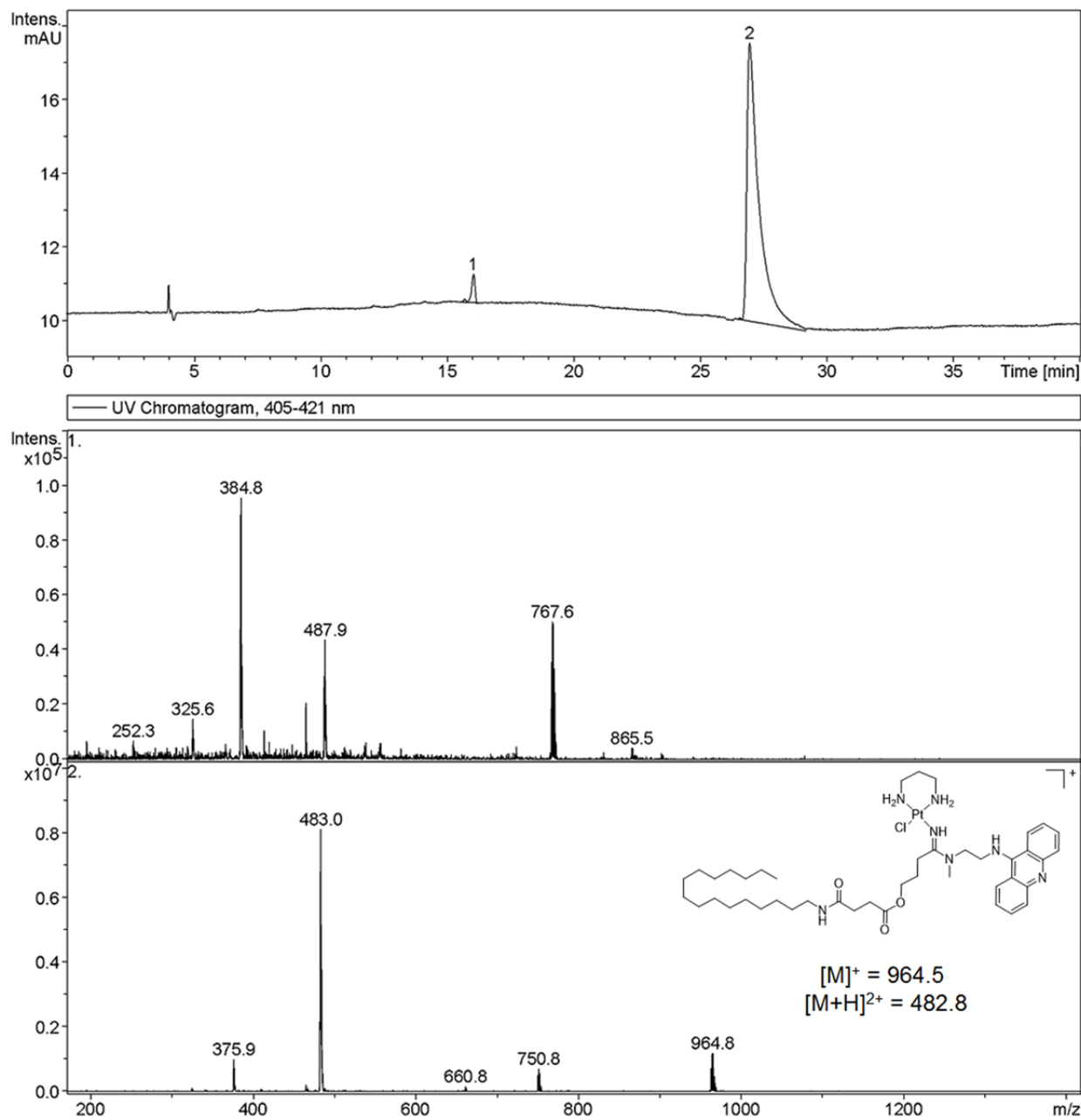


Figure S14. LC-MS analysis of the reaction mixture for the preparation of **P1-N2**.

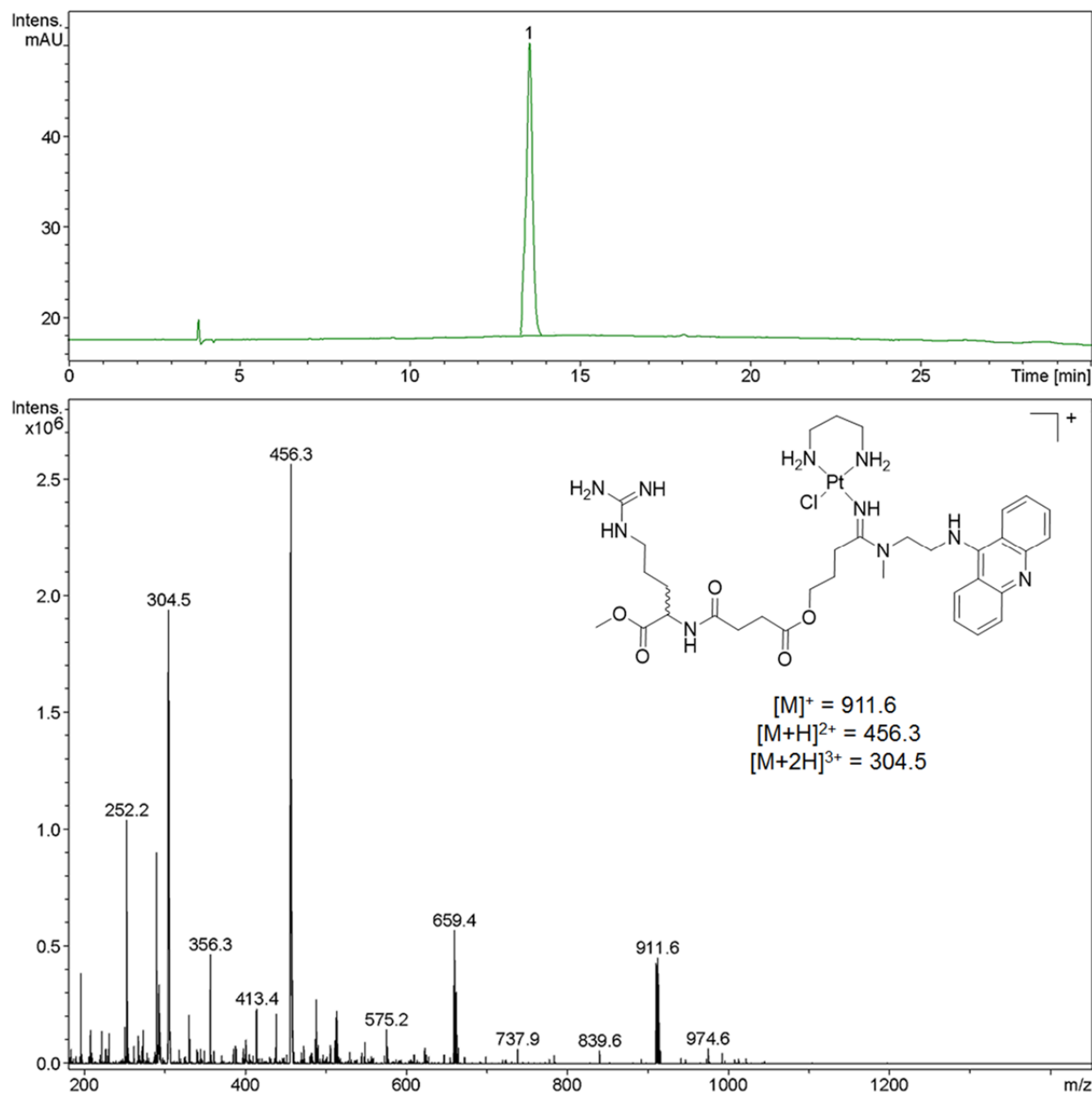


Figure S15. LC-MS analysis of the reaction mixture for the preparation of **P1-N4**.

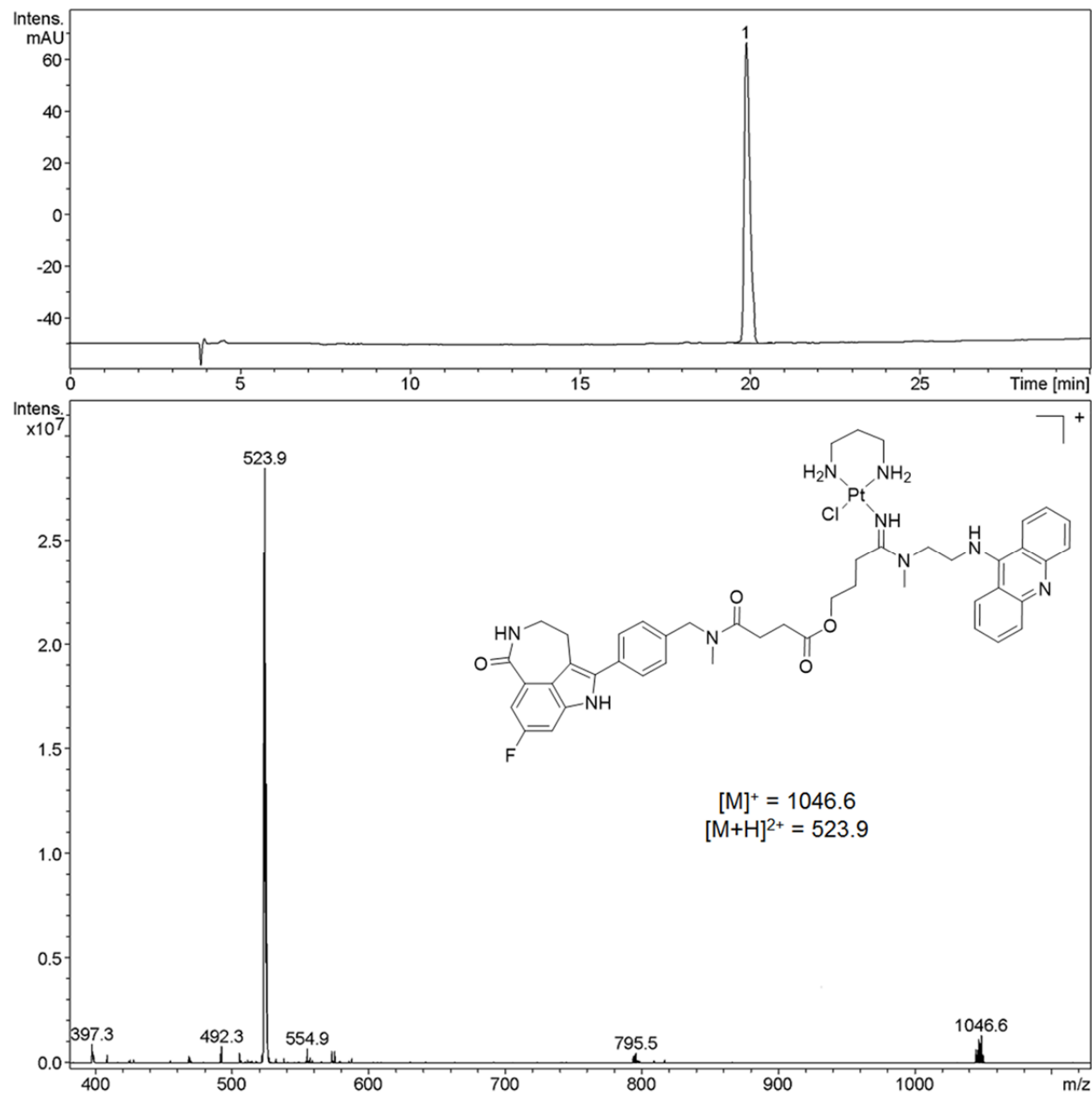


Figure S16. LC-MS analysis of the reaction mixture for the preparation of **P1-N5**.

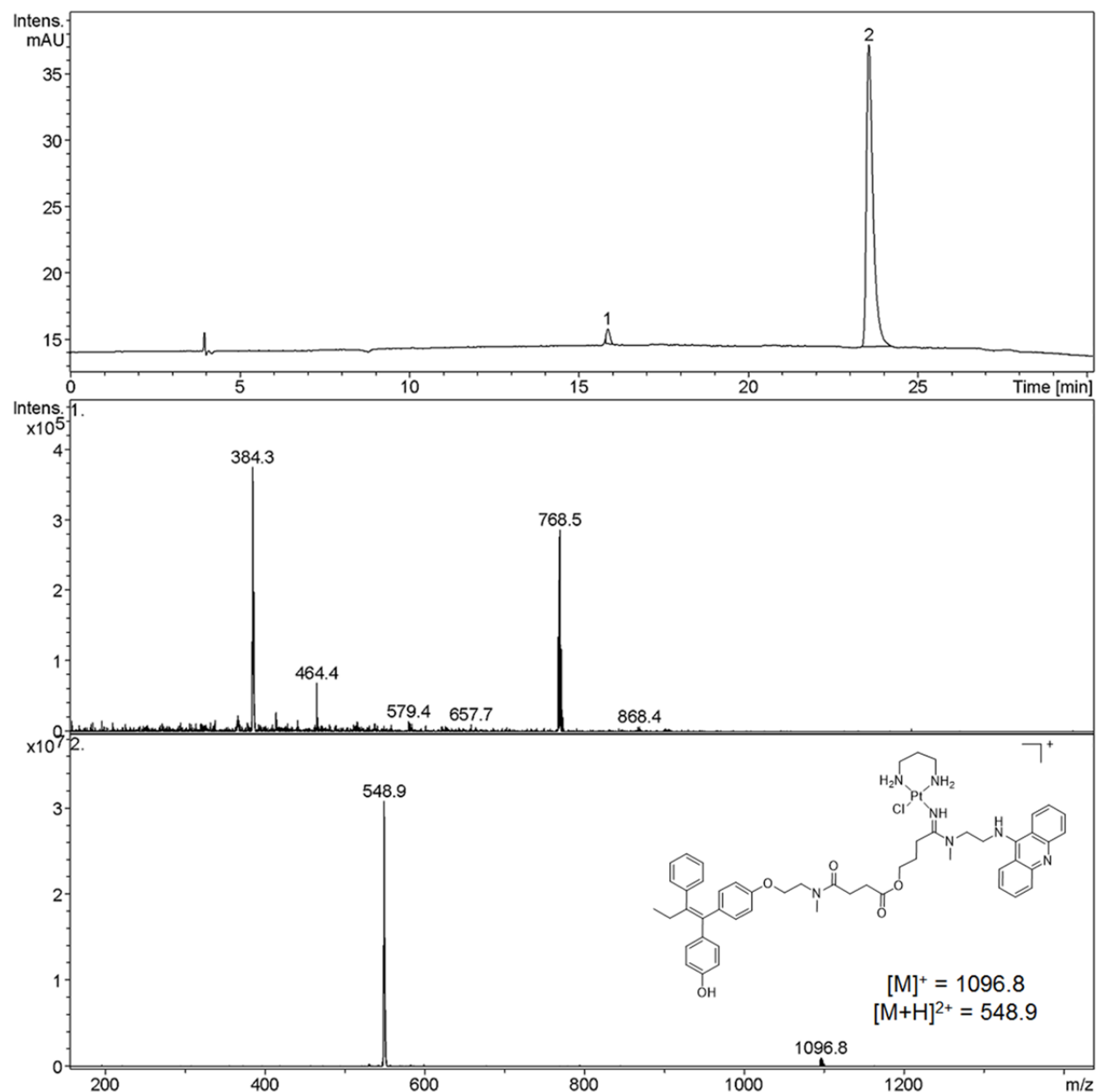


Figure S17. LC-MS analysis of the reaction mixture for the preparation of **P1-N6**.

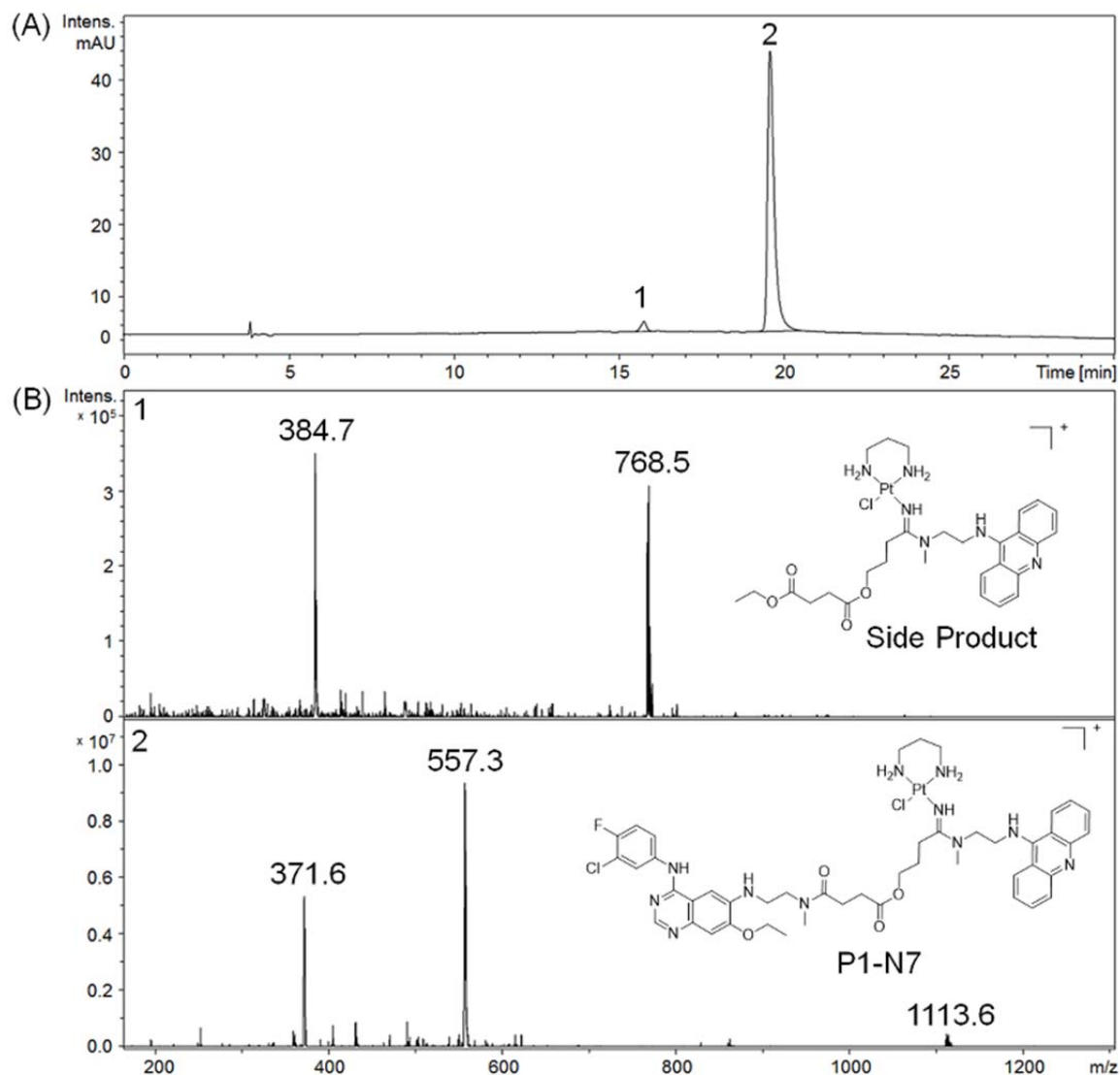


Figure S18. (A) Reverse-phase HPLC trace for the reaction of **P1** and **N7**. (B) ESMS spectrum recorded in positive-ion mode. Characteristic molecular and fragment ions for **P1-N7** are m/z $[M]^+$ 1113.6, $[M+H]^{2+}$ 557.3, $[M+2H]^{3+}$ 371.6.

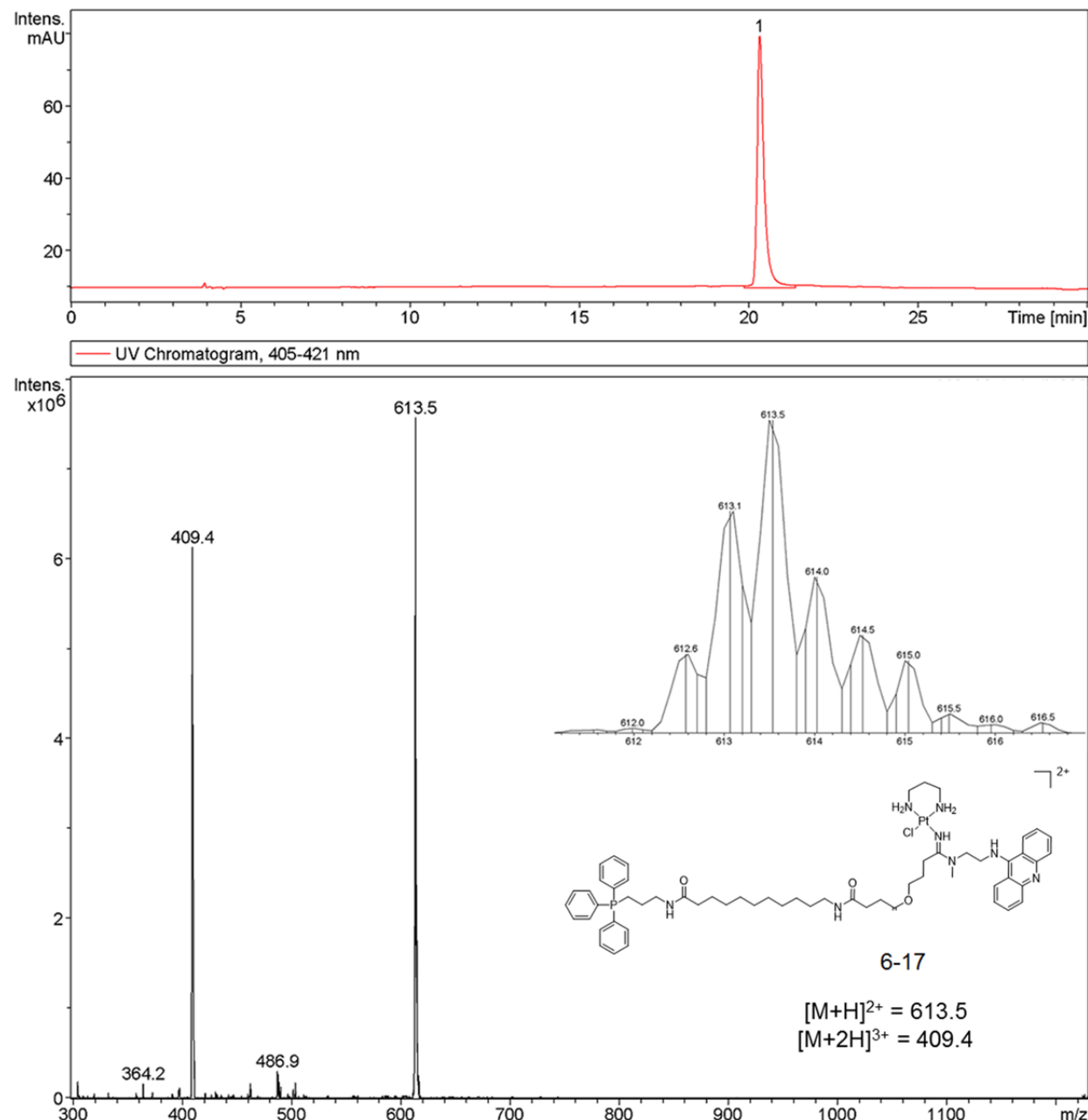


Figure S19. LC-MS analysis of the reaction mixture for the preparation of **P1-N9**.

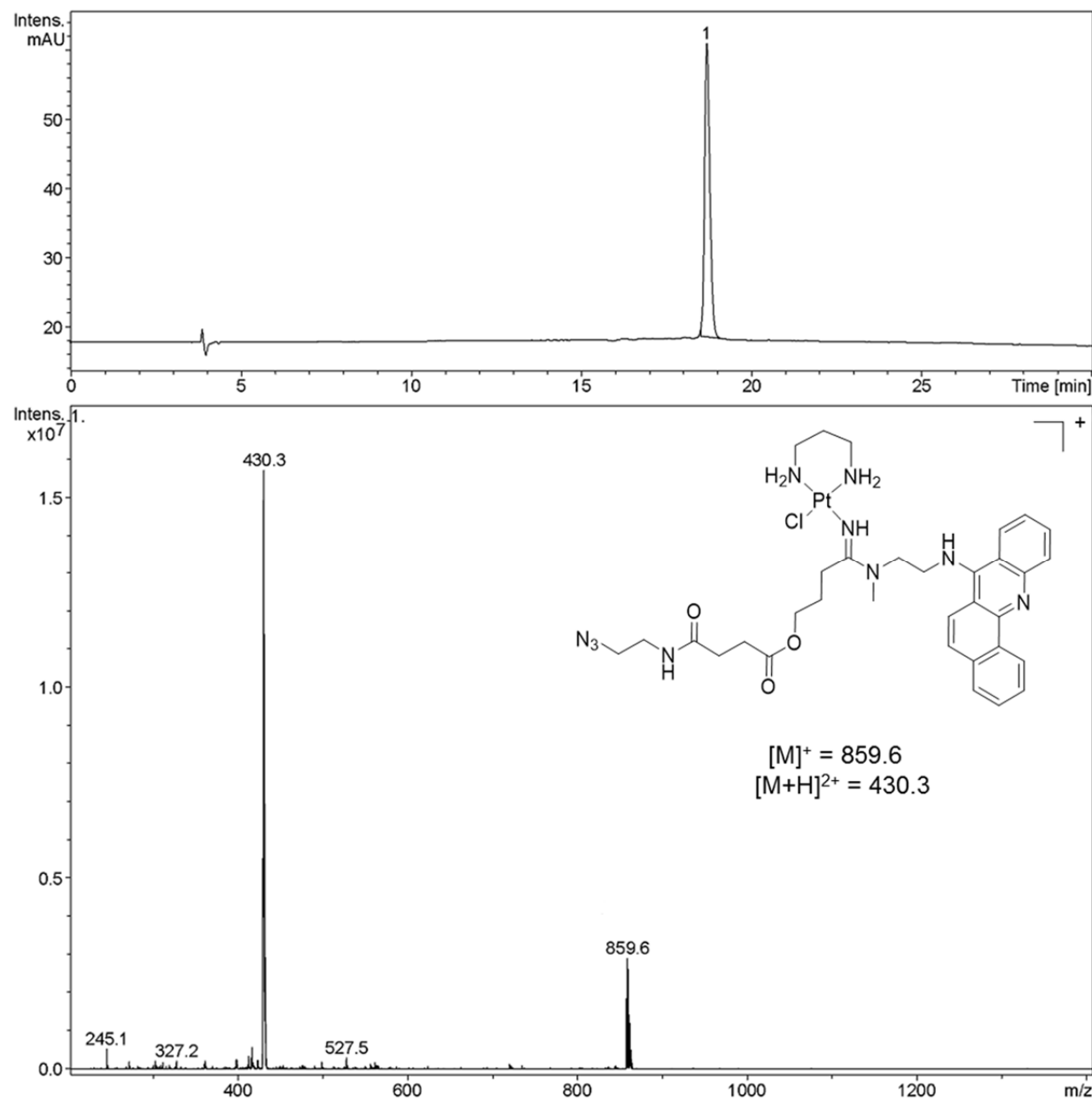


Figure S20. LC-MS analysis of the reaction mixture for the preparation of **P2-N1**.

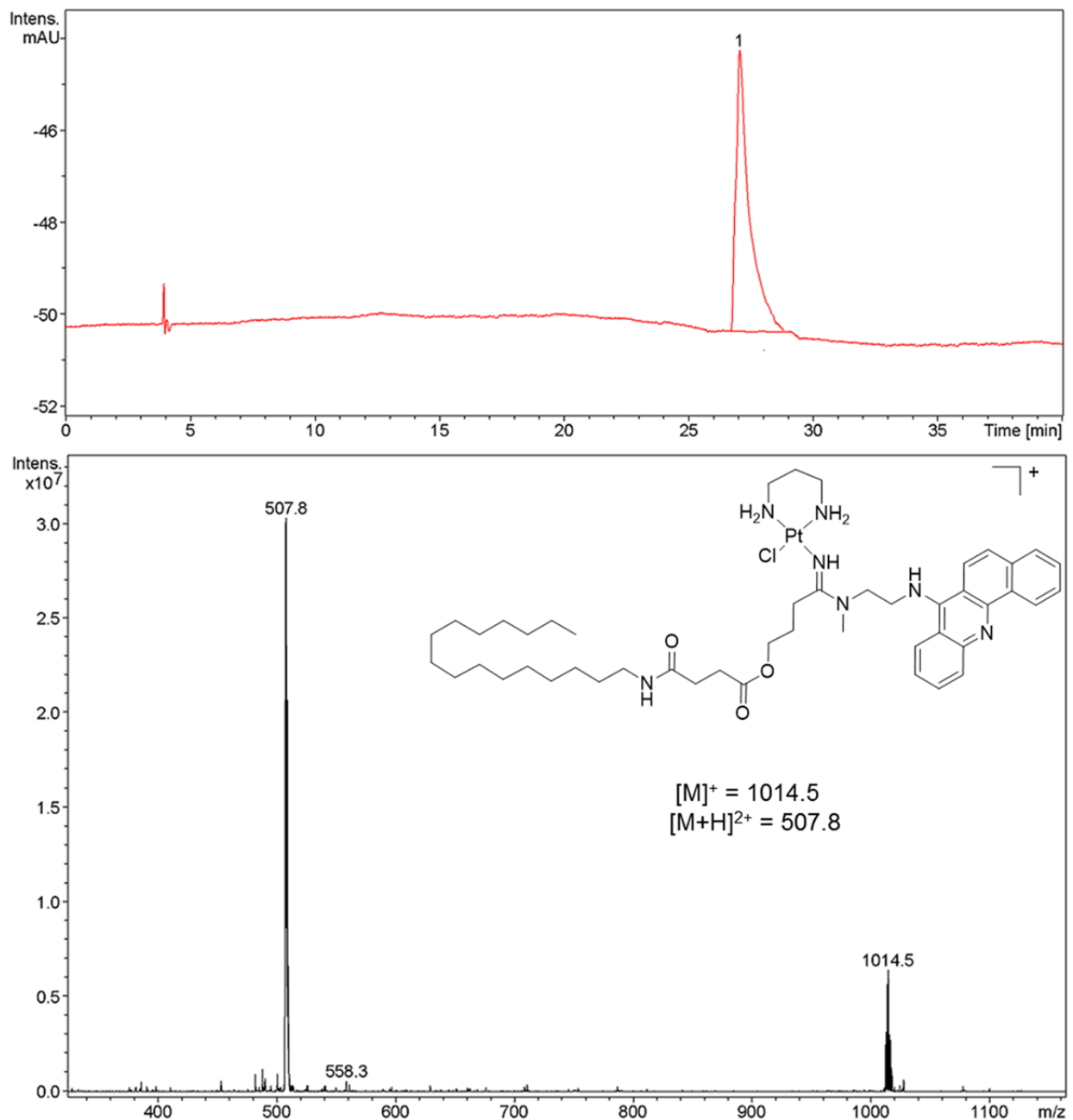


Figure S21. LC-MS analysis of the reaction mixture for the preparation of P2-N2.

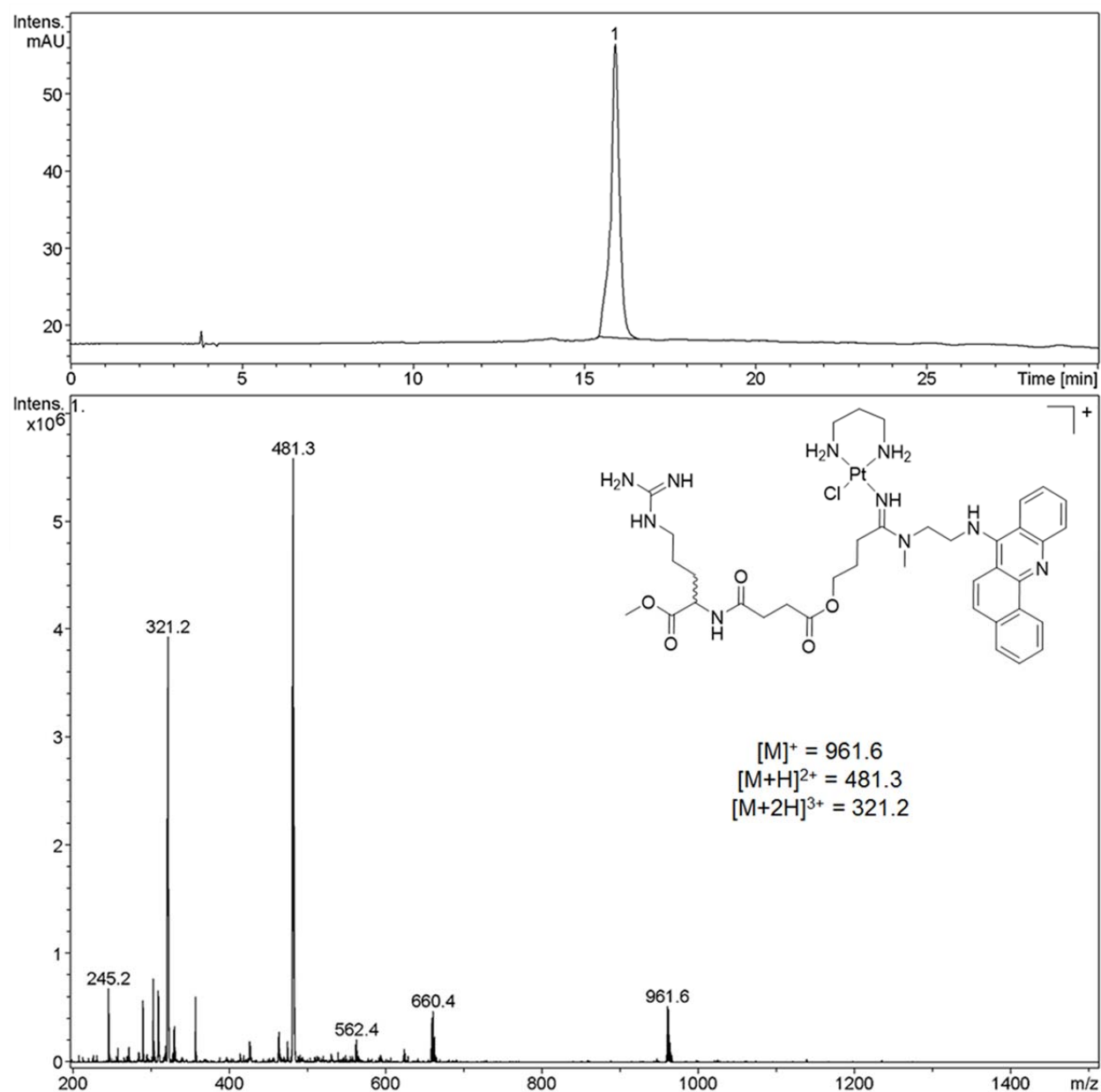


Figure S22. LC-MS analysis of the reaction mixture for the preparation of **P2-N4**.

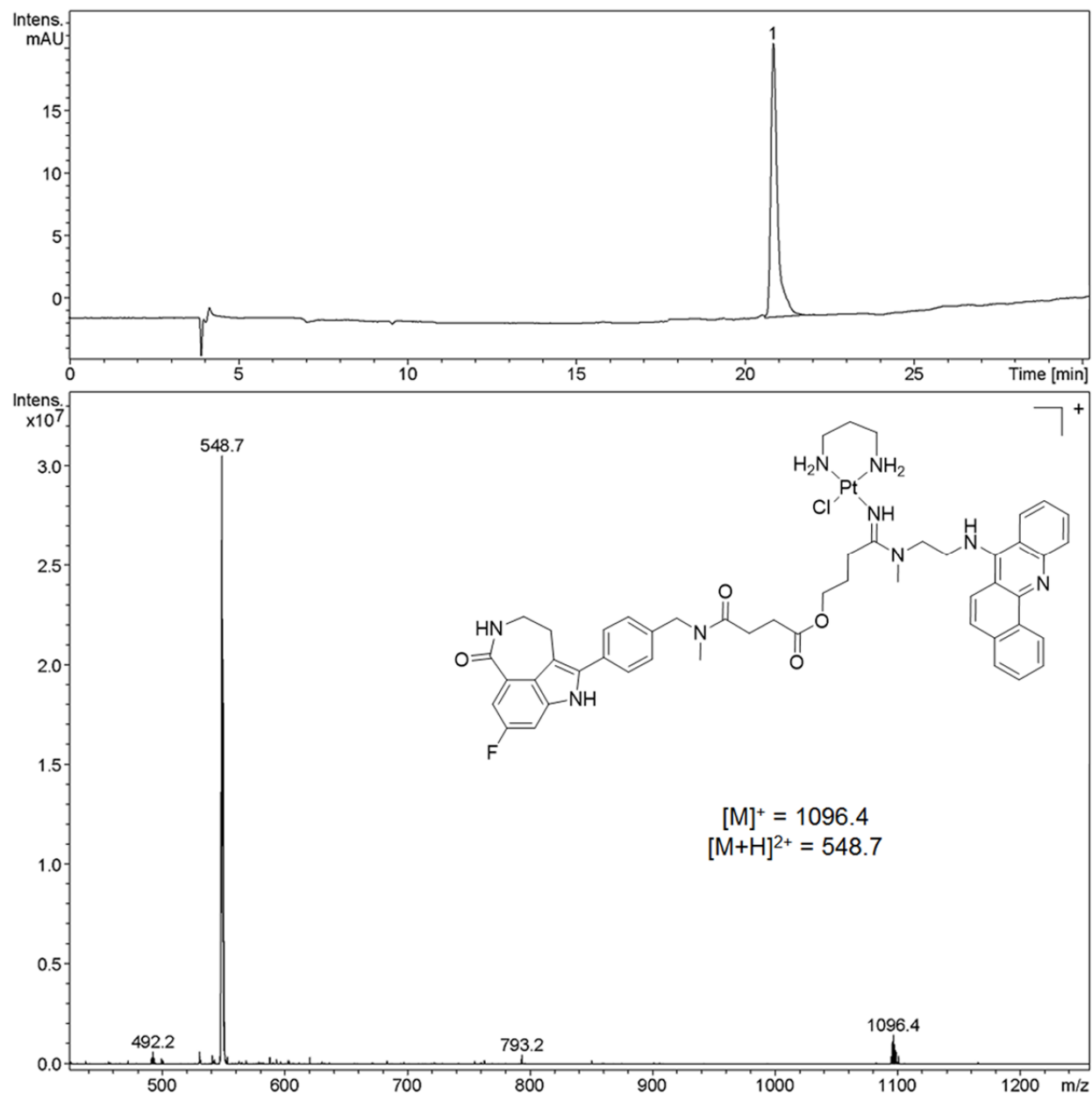


Figure S23. LC-MS analysis of the reaction mixture for the preparation of **P2-N5**.

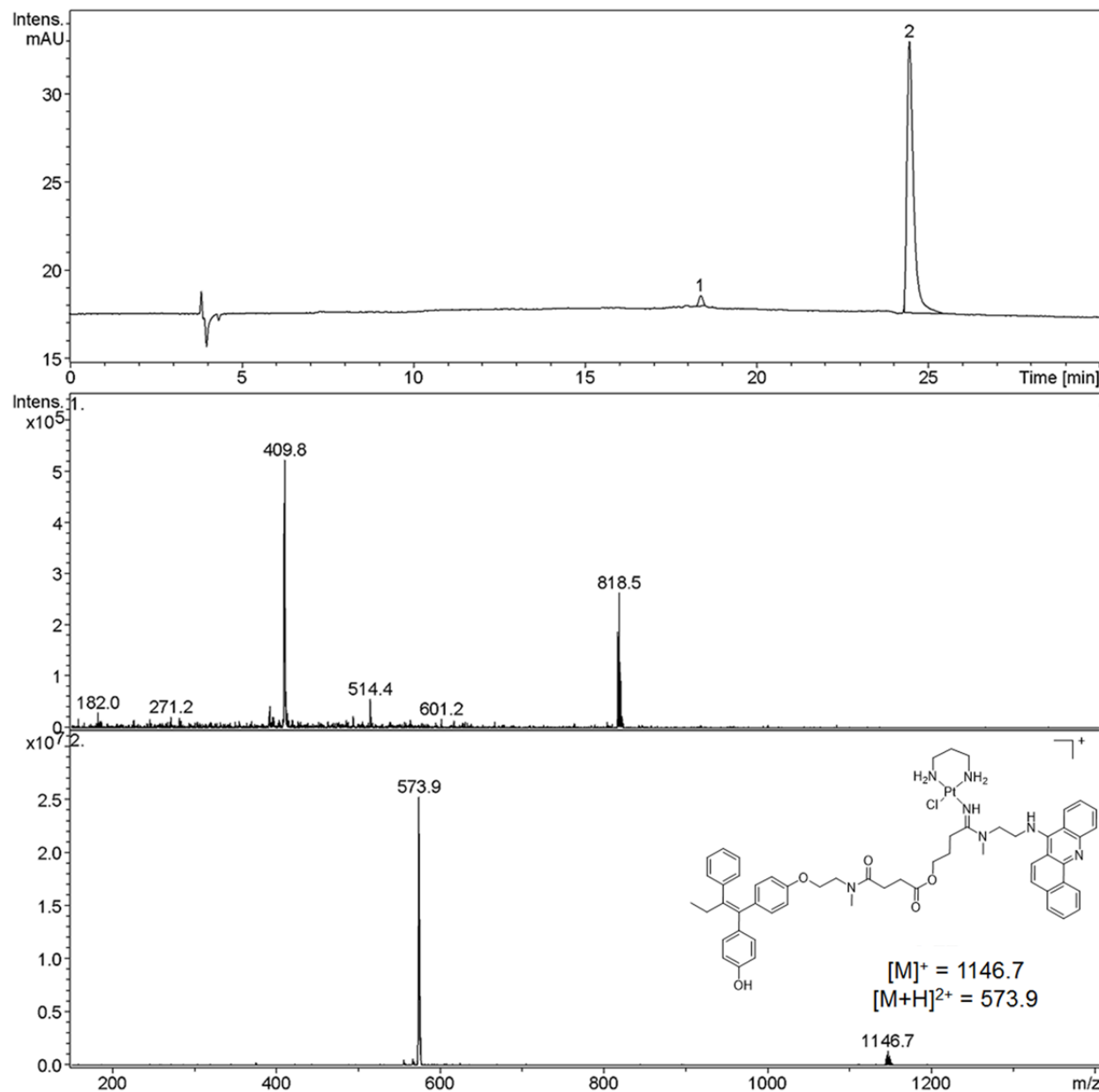


Figure S24. LC-MS analysis of the reaction mixture for the preparation of **P2-N6**.

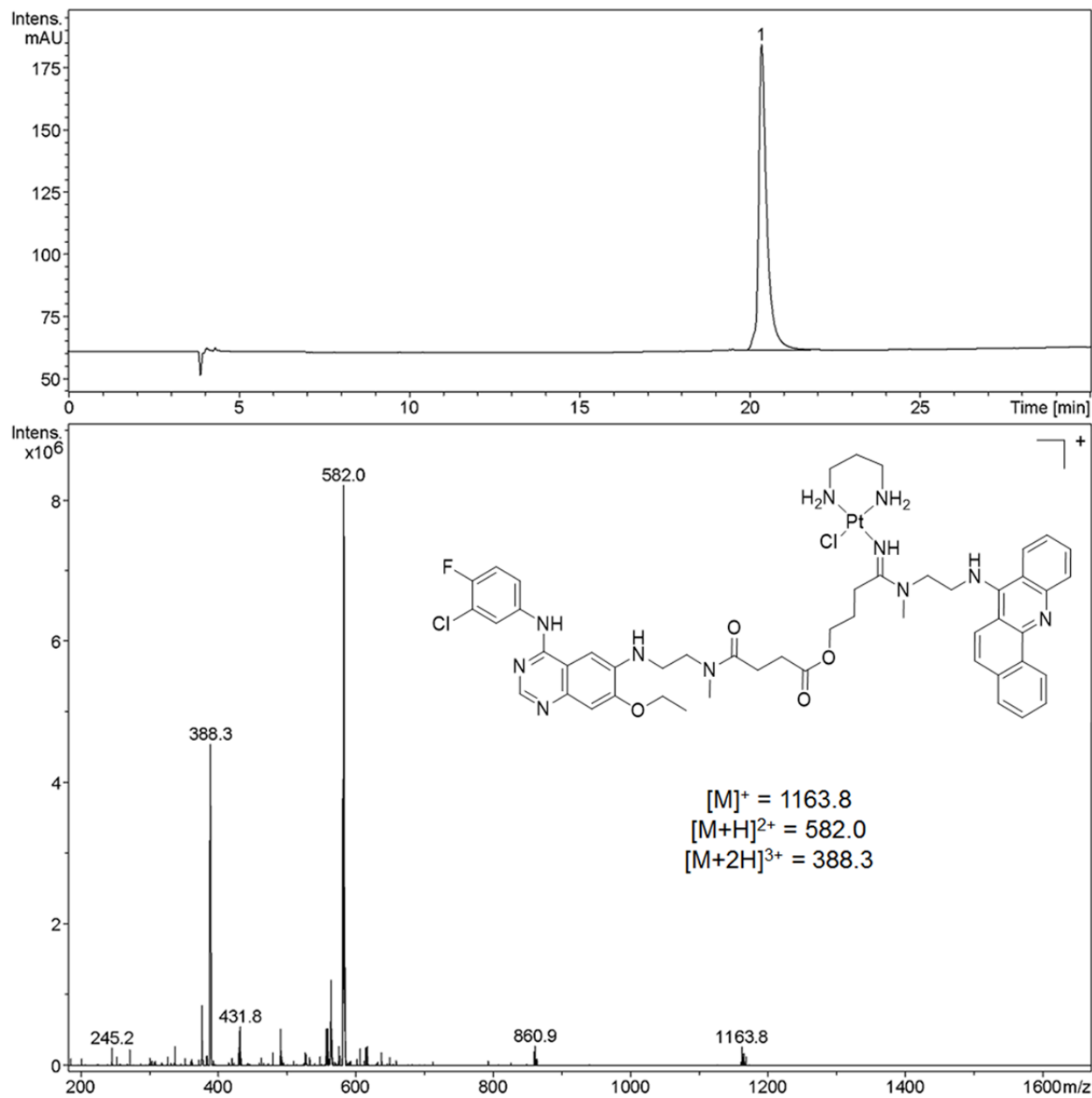


Figure S25. LC-MS analysis of the reaction mixture for the preparation of **P2-N7**.

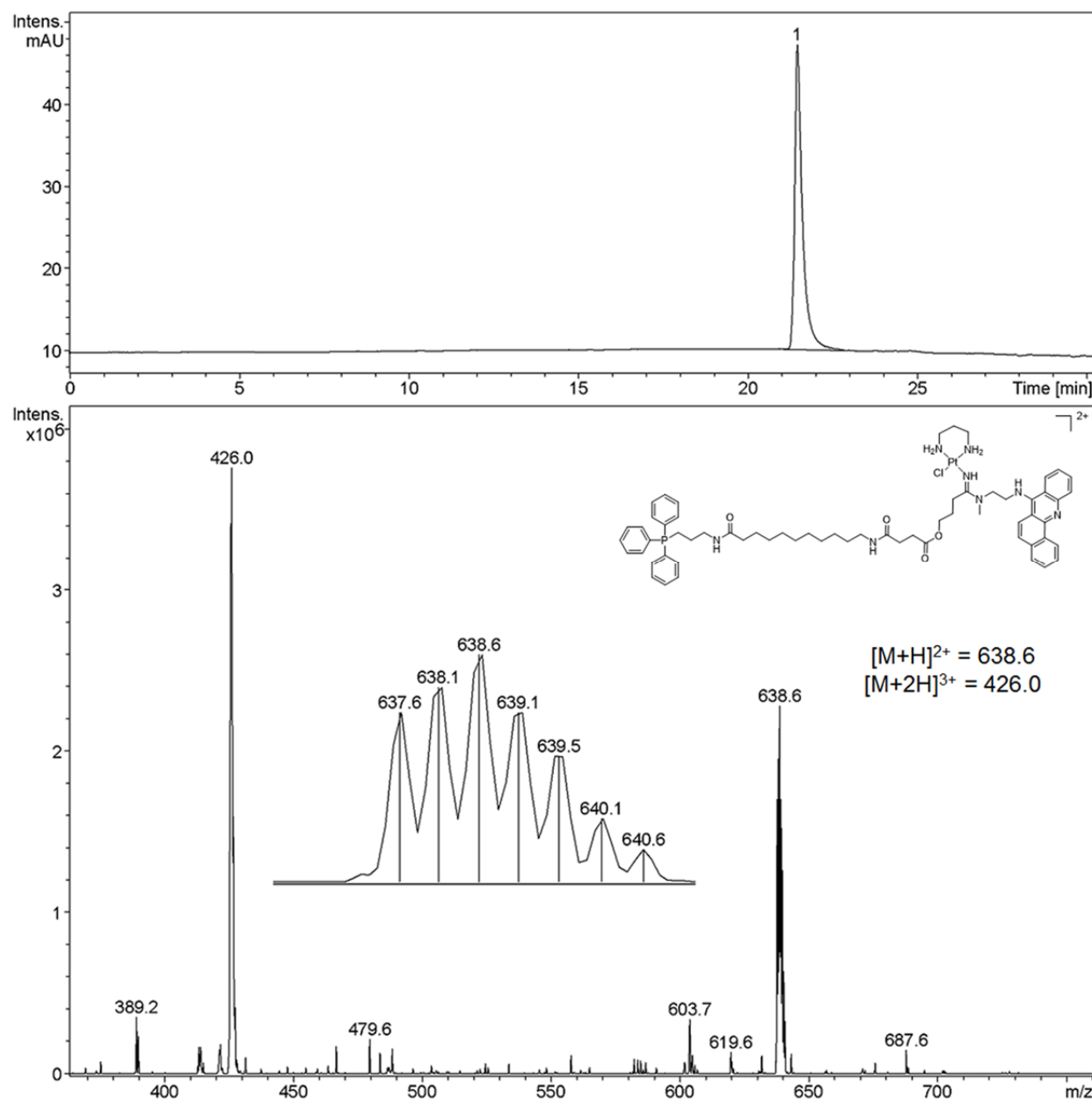


Figure S26. LC-MS analysis of the reaction mixture for the preparation of P2-N9.

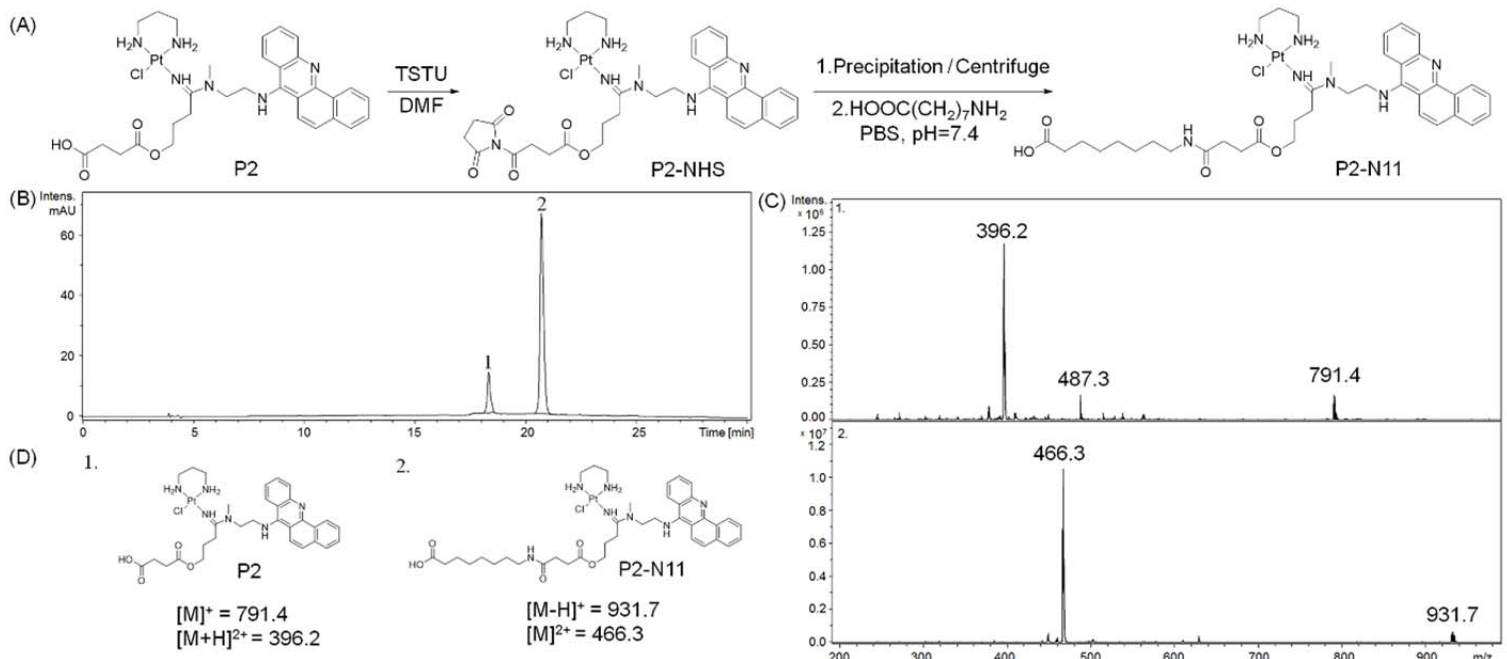


Figure S27. (A) “Two-step” synthesis of platinum-acridine conjugates under aqueous conditions. (B) Reverse-phase HPLC trace of the reaction mixture for the preparation of **P2-N11**. (C) ESMS spectrum of **P2** and target conjugate **P2-N11** recorded in positive-ion mode. (D) Structures and characteristic molecular ions and fragment ions (m/z) for **P2** and **P2-N11**.

S.4. LC-MS ANALYSIS OF ESTER REACTIVITY

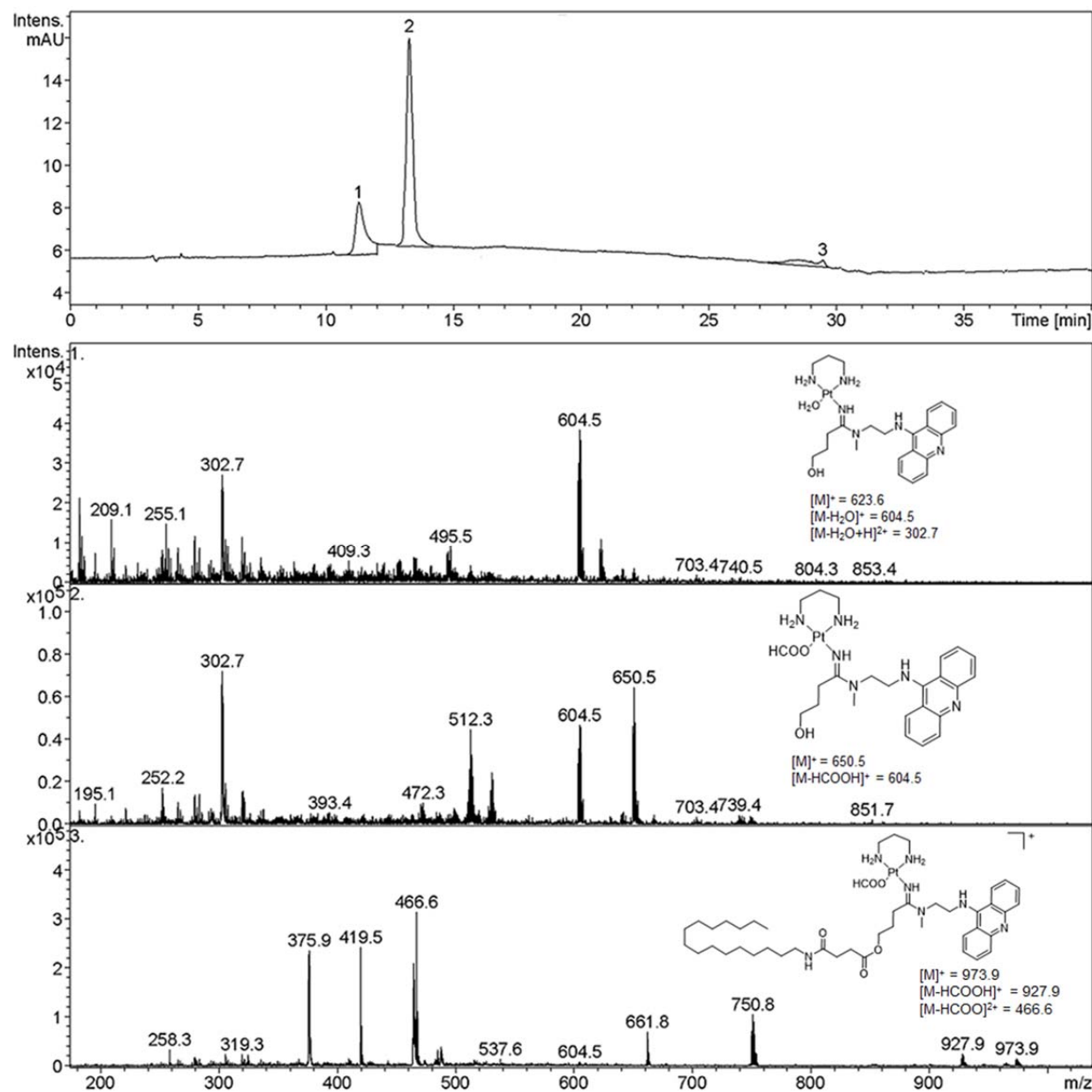


Figure S28. LC-ESMS analysis of the mixture of compound **P1-N2** in phosphate buffer (PB, pH 7.4) incubated at 37 °C.

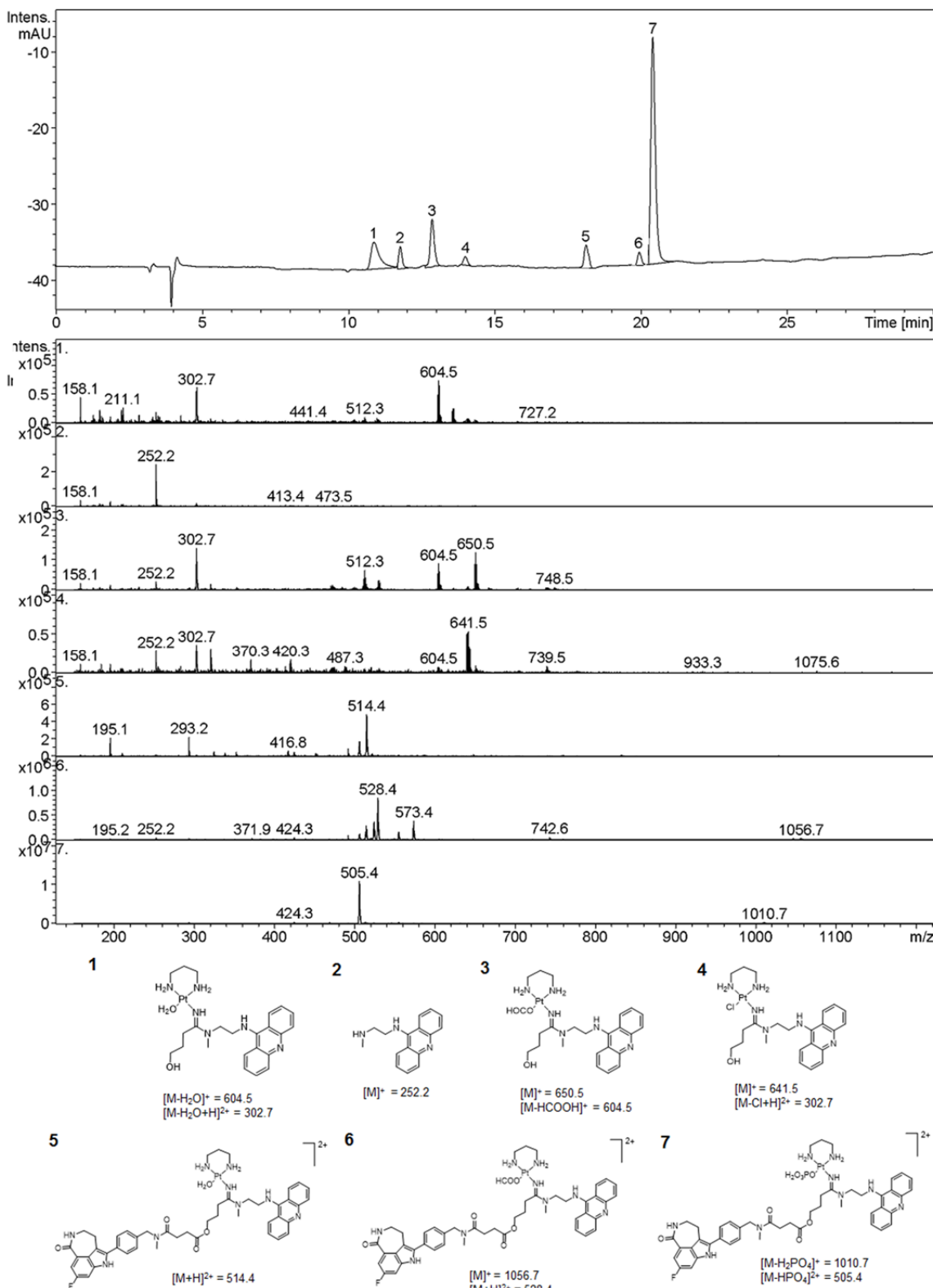


Figure S29. LC-ESMS analysis of the mixture of compound **P1-N5** in phosphate buffer (PB, pH 7.4) incubated at 37 °C.

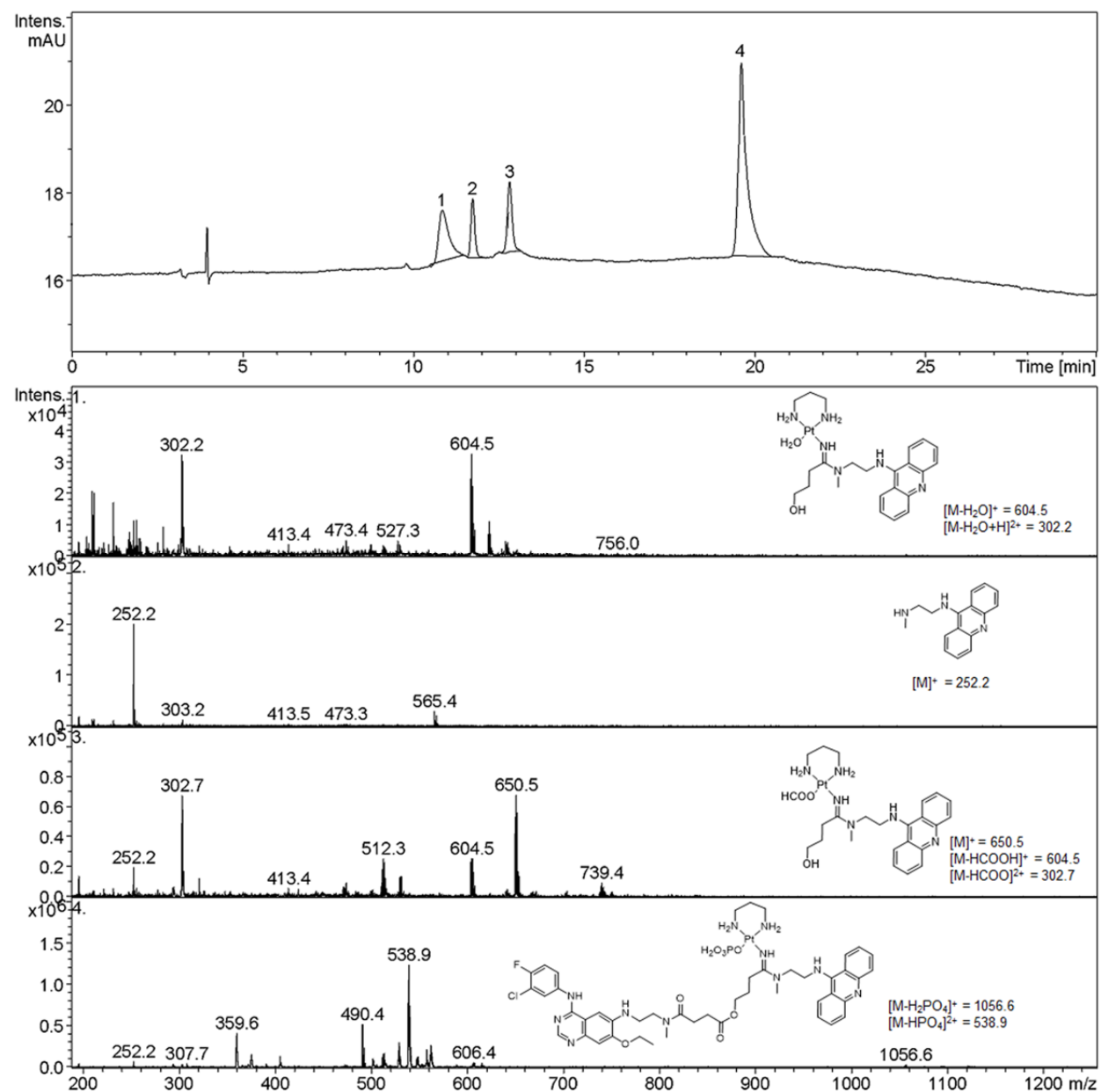


Figure S30. LC-ESMS analysis of the mixture of compound **P1-N7** in phosphate buffer (PB, pH 7.4) incubated at 37 °C.

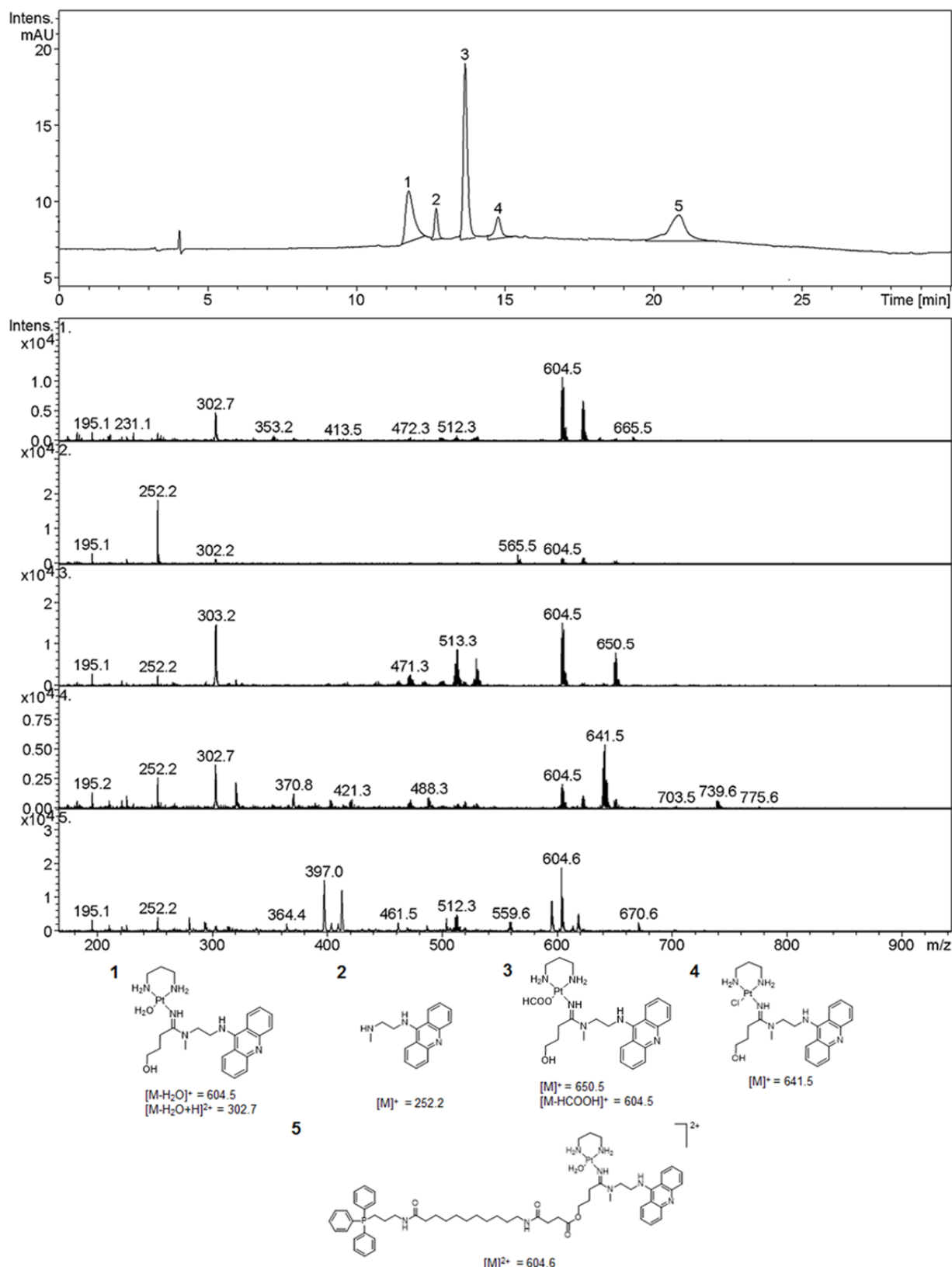


Figure S31. LC-ESMS analysis of the mixture of compound **P1-N9** in phosphate buffer (PB, pH 7.4) incubated at 37 °C.

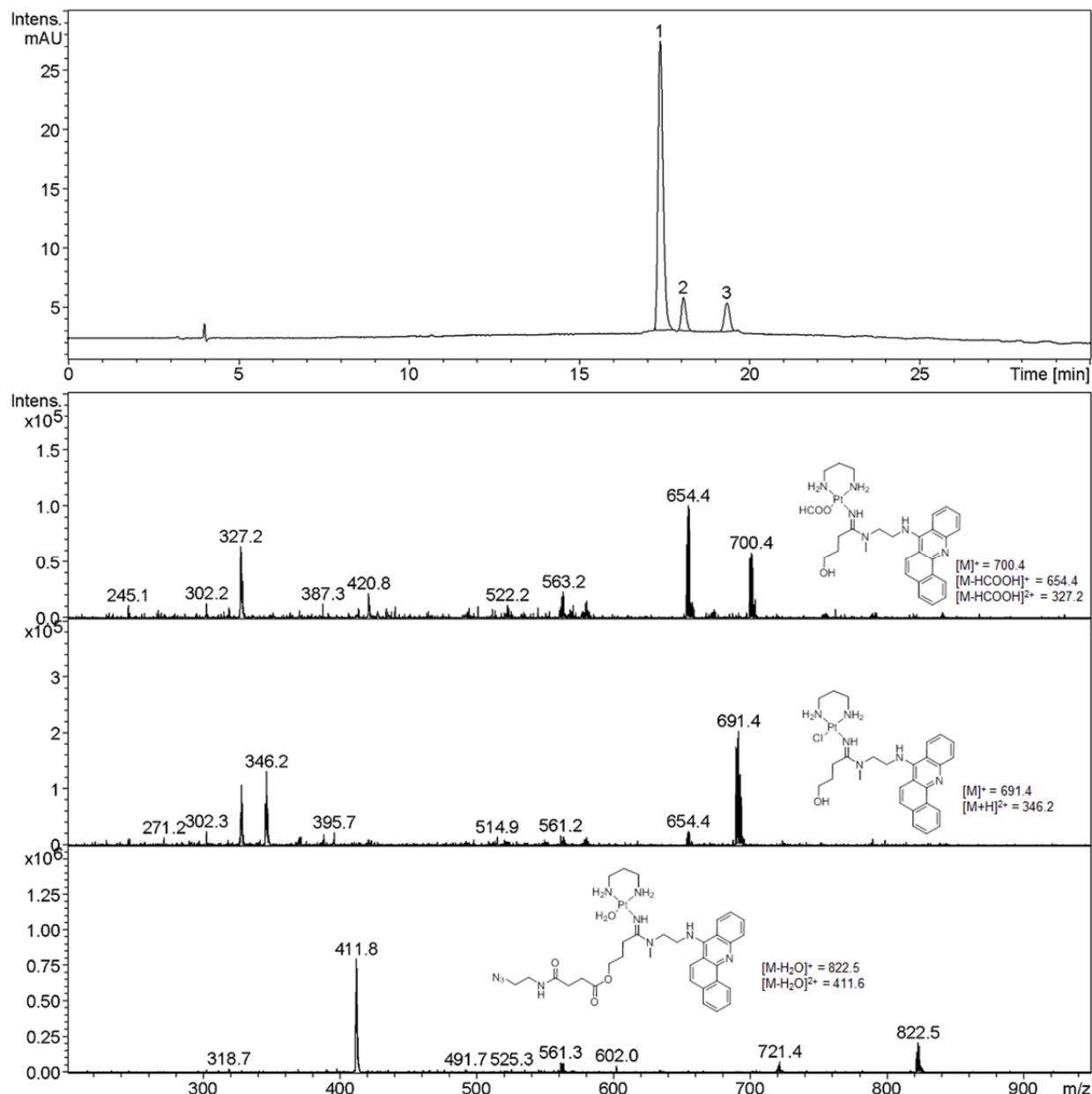


Figure S32. LC-ESMS analysis of the mixture of compound **P2-N1** in phosphate buffer (PB, pH 7.4) incubated at 37 °C.

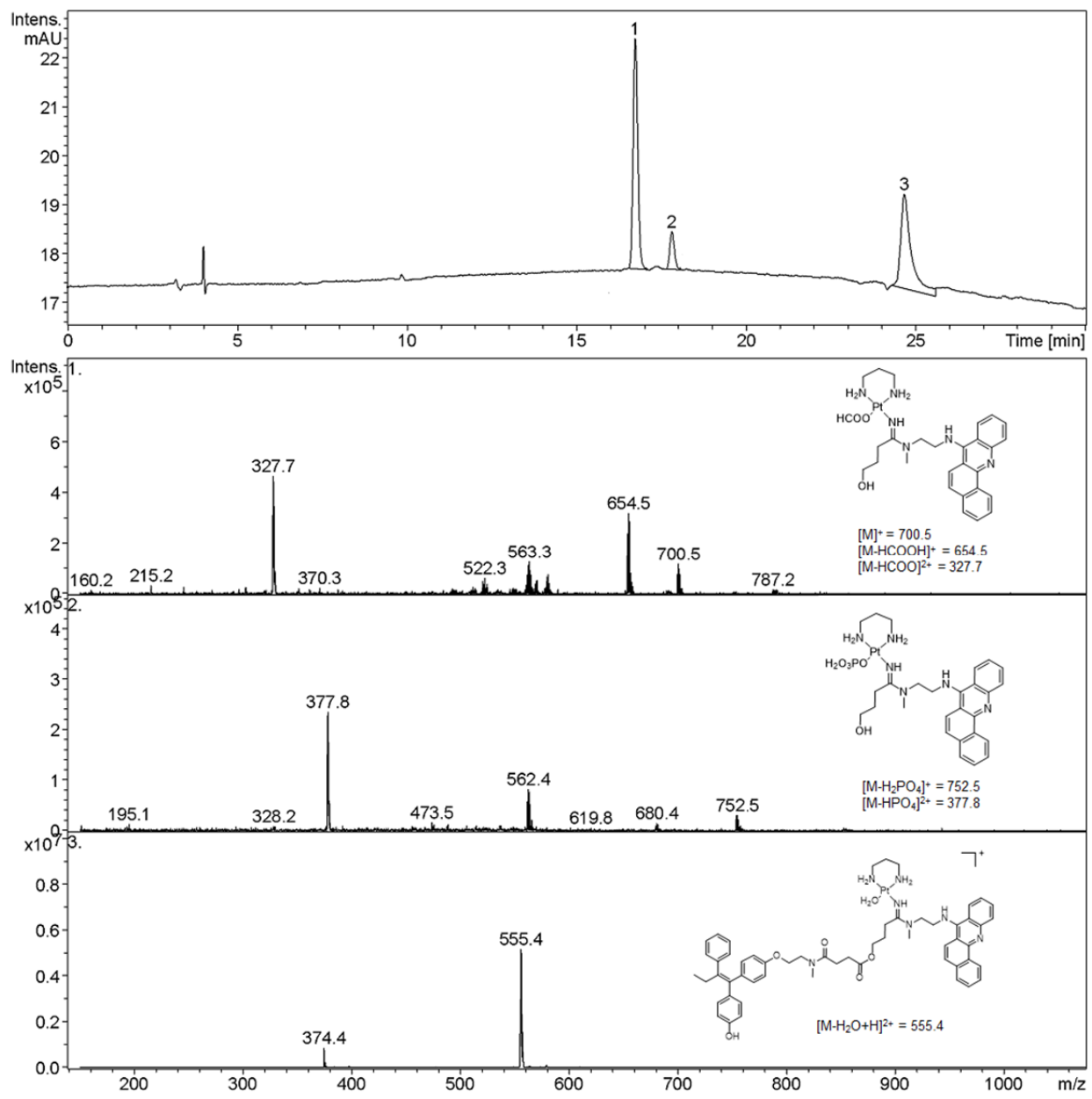


Figure S33. LC-ESMS analysis of the mixture of compound **P2-N6** in phosphate buffer (PB, pH 7.4) incubated at 37 °C.

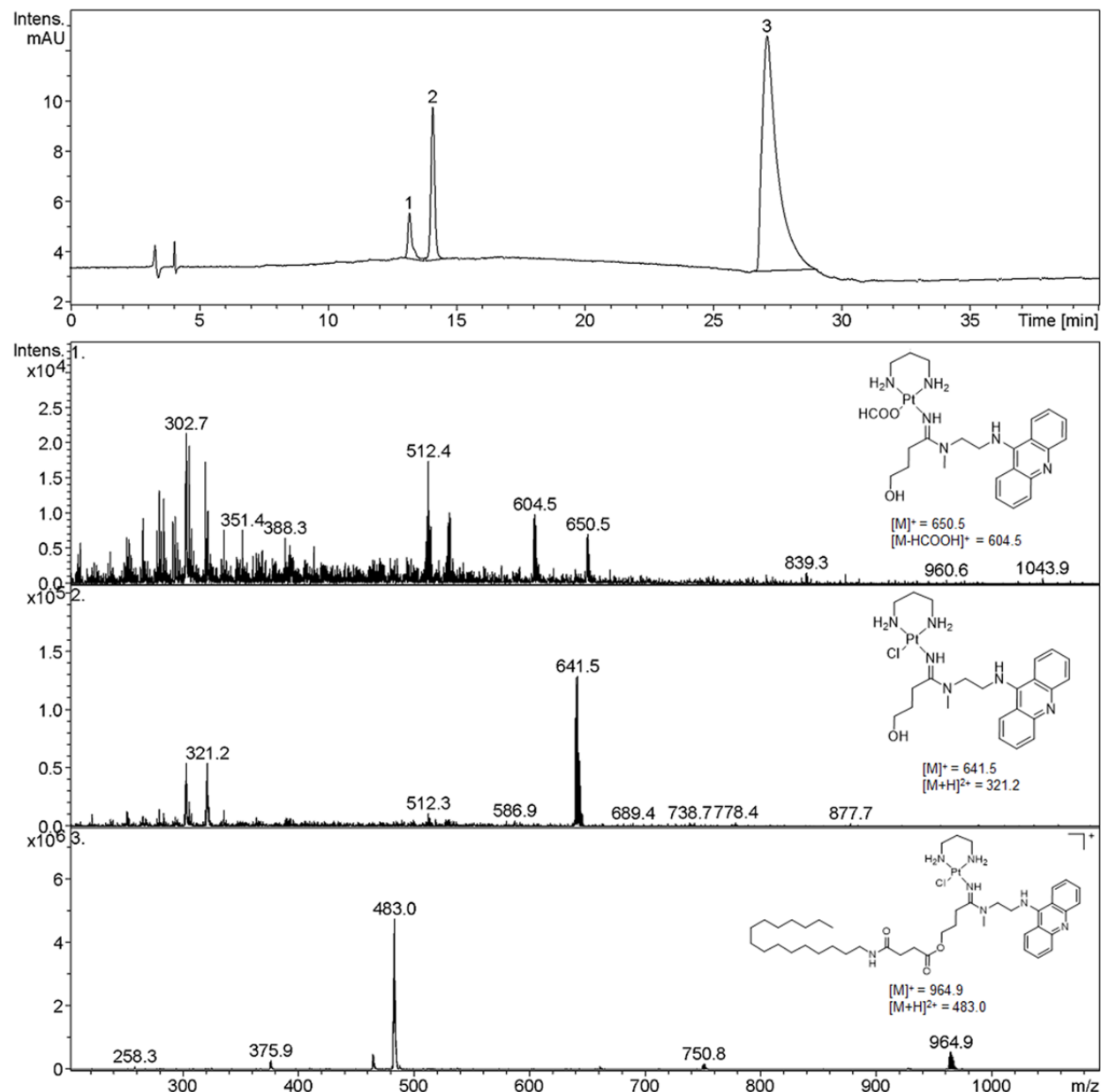


Figure S34. LC-ESMS analysis of the mixture of compound **P1-N2** in phosphate buffered saline (PBS, pH 7.4) incubated at 37 °C.

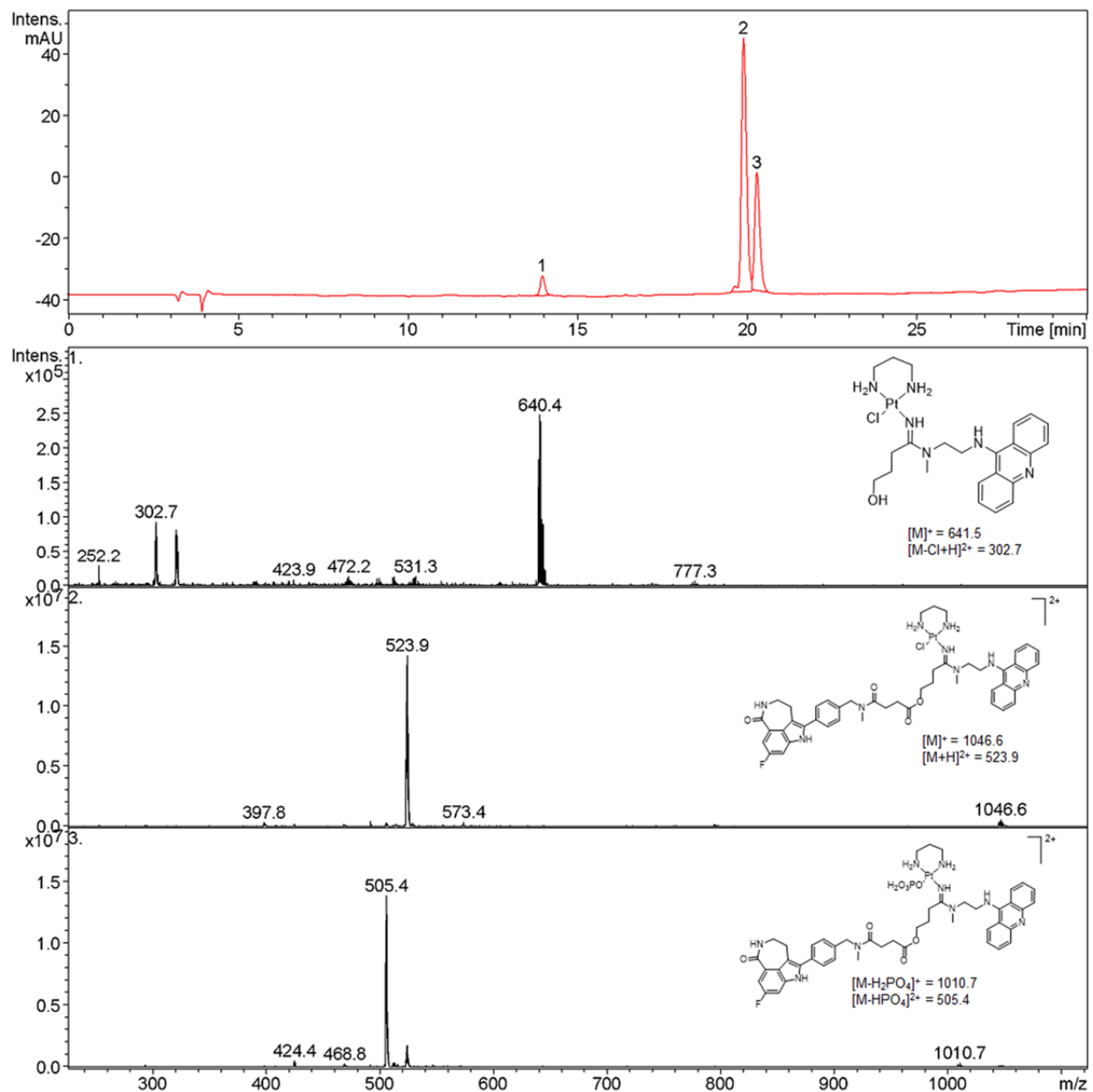


Figure S35. LC-ESMS analysis of the mixture of compound **P1-N5** in phosphate buffered saline (PBS, pH 7.4) incubated at 37 °C.

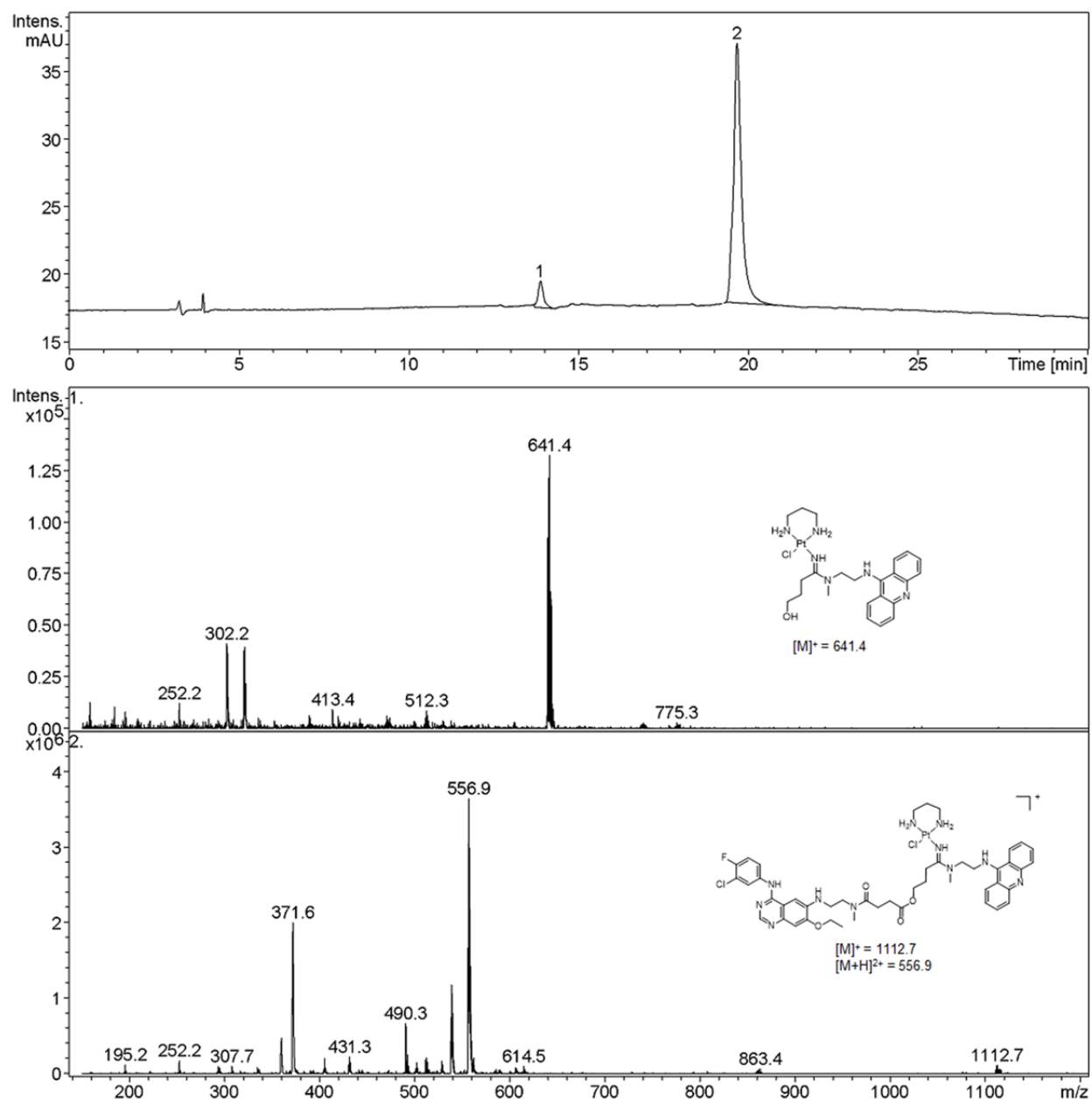


Figure S36. LC-ESMS analysis of the mixture of compound **P1-N7** in phosphate buffered saline (PBS, pH 7.4) incubated at 37 °C.

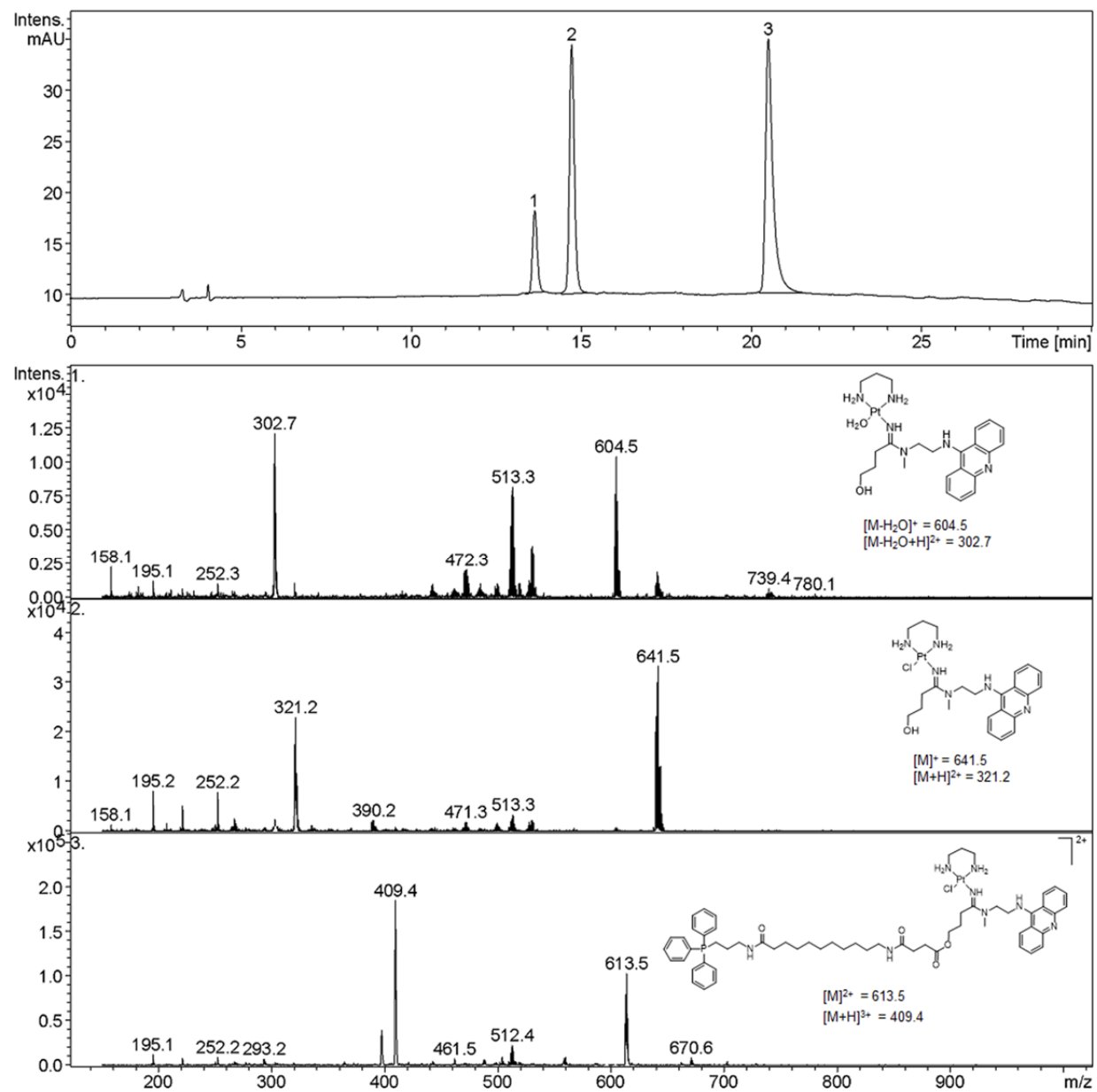


Figure S37. LC-ESMS analysis of the mixture of compound **P1-N9** in phosphate buffered saline (PBS, pH 7.4) incubated at 37 °C.

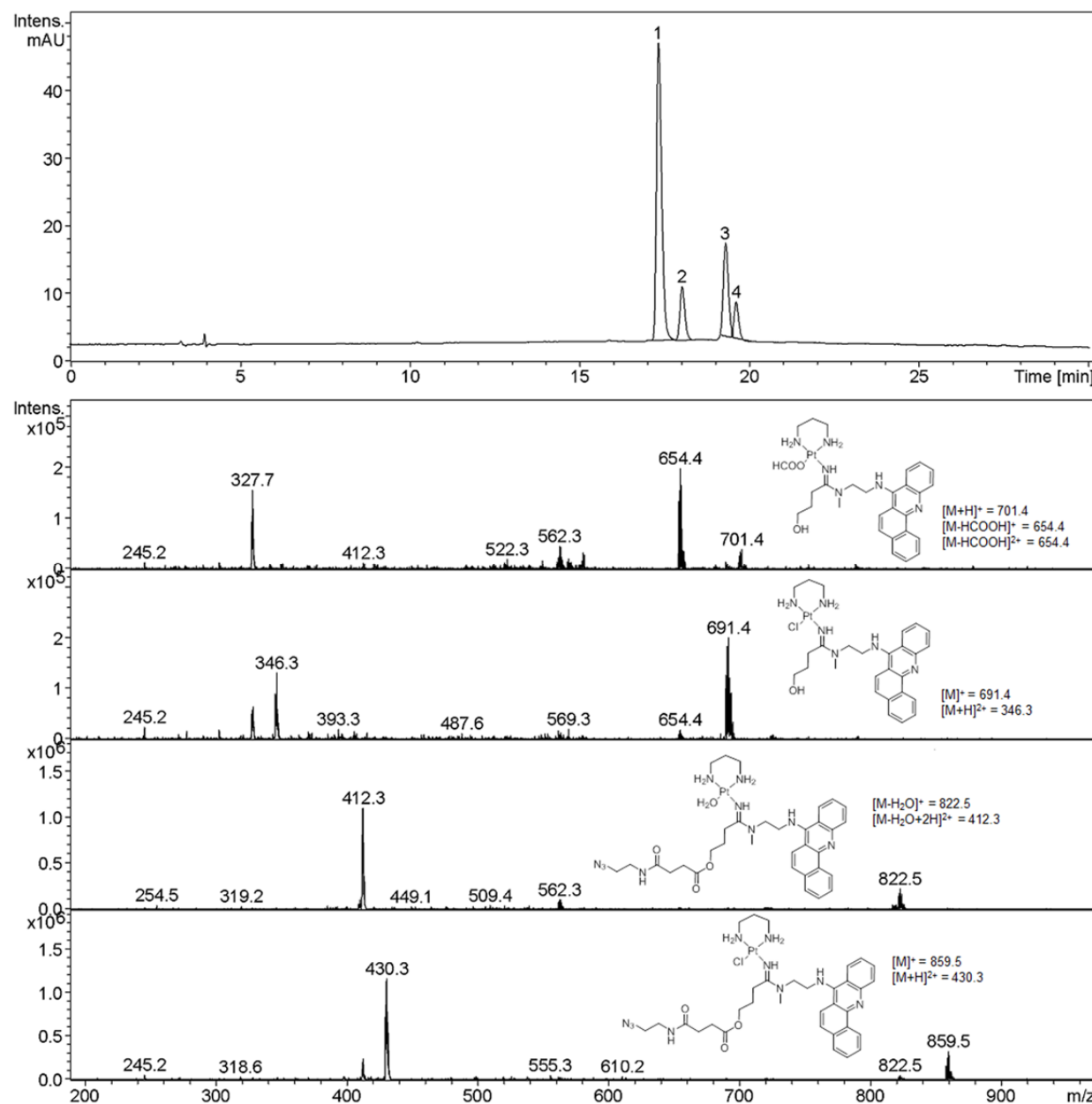


Figure S38. LC-ESMS analysis of the mixture of compound **P2-N1** in phosphate buffered saline (PBS, pH 7.4) incubated at 37 °C.

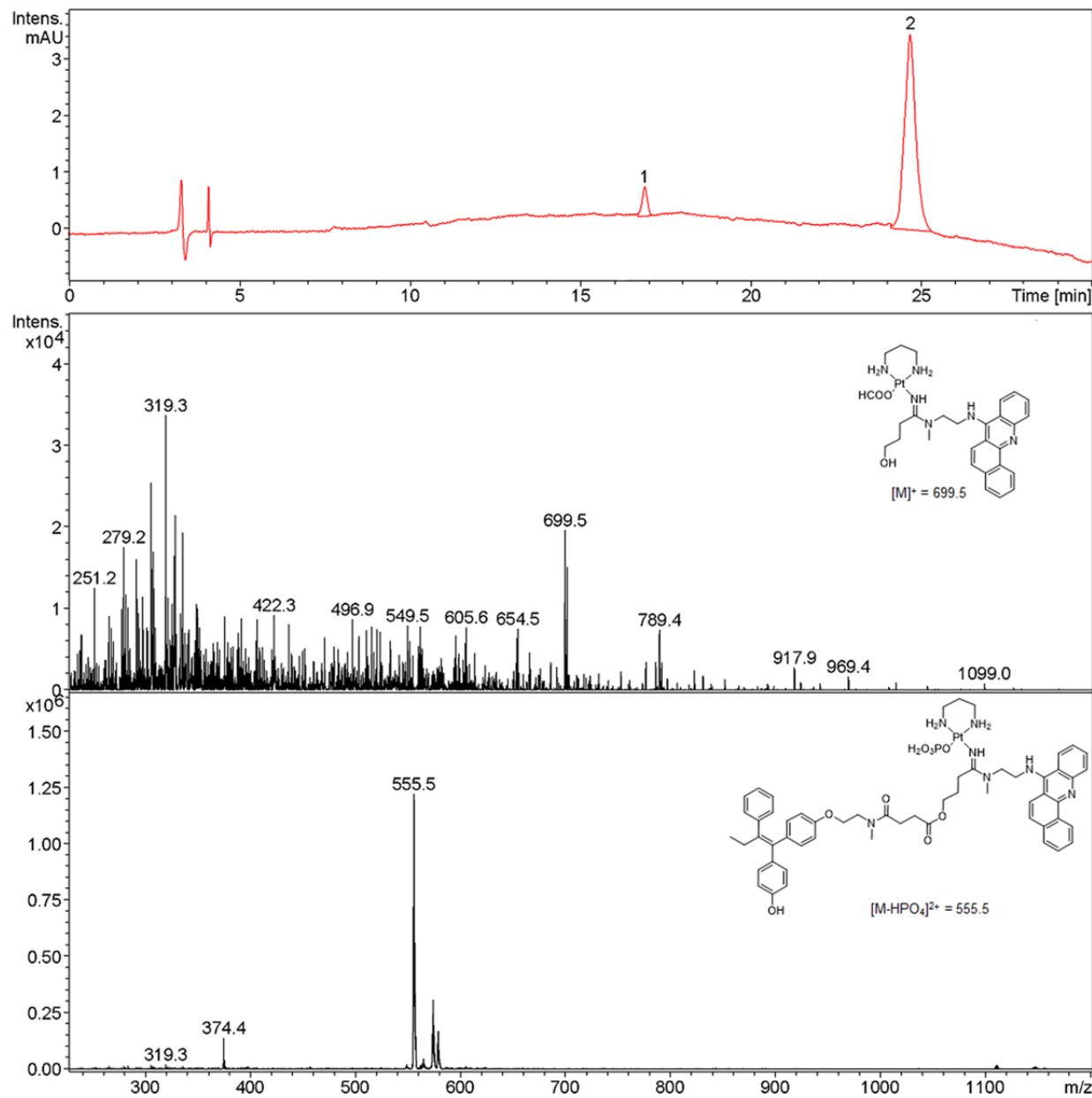


Figure S39. LC-ESMS analysis of the mixture of compound **P2-N6** in phosphate buffered saline (PBS, pH 7.4) incubated at 37 °C.

Table S1. Conversion Yields and HR-ESMS Results for Conjugates

Compd	Conjugate structures	Conv. (%) \pm S.D. ^a	Calculated [M] ⁺	Observed [M] ⁺
P1-N1 P2-N1		98.9 \pm 1.4 98.1 \pm 1.7	808.2778 858.2934	808.2786 858.2940
P1-N2 P2-N2		96.6 \pm 1.2 96.9 \pm 2.3	963.4955 1013.5111	963.4954 1013.5125
P1-N4 P2-N4		99.5 \pm 1.9 99.4 \pm 1.1	910.3458 960.3615	910.3466 960.3610
P1-N5 P2-N5		96.4 \pm 2.5 98.9 \pm 1.4	1045.3619 1095.3776	1045.3645 1095.3784
P1-N6 P2-N6		97.1 \pm 2.3 96.7 \pm 0.9	1095.4227 1145.4383	1095.4242 1145.4391
P1-N7 P2-N7		97.8 \pm 1.5 96.4 \pm 2.5	1111.3604 1162.3760	1111.3615 1162.3744
P1-N9 P2-N9		99.8 \pm 0.2 99.7 \pm 0.5	612.7688 637.7766 (2+) ^b	612.7696 637.7769 (2+) ^b

^a Each reaction was performed in triplicate. The conversion yields were determined from HPLC traces recorded at an acridine-specific wavelength. Reactions with conversion yields lower than 90% are not reported. ^b Singly charged [M]⁺ not observed in positive-ion mode. The additional fused ring in the benz[cl]acridine derivatives (**P2**) is shown as dashed bonds.

Table S2. Summary of Coupling Reagents Used

Acronym, Common Name	System. Nomenclature	Structure
EDC	<i>N</i> -(3-Dimethylaminopropyl)- <i>N'</i> -ethylcarbodiimide hydrochloride	
DCC	<i>N,N'</i> -Dicyclohexylcarbodiimide	
CDI	1,1'-Carbonyldiimidazole	
PyBOP	Benzotriazol-1-yl-oxytritypyrrolidinophosphonium hexafluorophosphate	
COMU	1-[(1-Cyano-2-ethoxy-2-oxoethylideneaminoxy)-dimethylamino-morpholinomethylene] methanaminium hexafluorophosphate	
TSTU	O-(<i>N</i> -Succimidinyl)- <i>N,N,N',N'</i> -tetramethyluronium tetrafluoroborate	
HBTU	<i>O</i> -(Benzotriazol-1-yl)- <i>N,N,N',N'</i> -tetramethyluronium hexafluorophosphate	